Driver and Sensor Node Selection Strategies Optimizing the Controllability Properties of Complex Dynamical Networks

Ph.D Thesis

Francesco Lo Iudice

Tutor

Ch.mo Prof. Franco Garofalo

University of Naples Federico II
Department of Electrical Engineering and Information Technology
Naples, Italy
2016

Contents

List of Figures

List of Tables

Abstract

In recent years, complex networks have attracted the attention of researchers throughout the fields of science due to their ubiquity in natural and artificial settings. While the spontaneous emergence of collective behavior has been thoroughly studied, and has inspired researchers in the design of control strategies able to reproduce it in artificial scenarios, our ability to arbitrarily affect the behavior of complex networks is still limited. To start filling this void, in the past five years, researchers have focused on the preliminary condition of selecting the nodes where input signals have to be injected so to ensure complete controllability of complex networks. Unfortunately, the scale of complex networks is such that more often than not too many input signals are required to arbitrarily modify the behavior of all the nodes of a network. Departing from the idea that achieving complete controllability of complex networks is a chimera, in this thesis, we present a comprehensive toolbox of input selection algorithms so to ensure controllability of the largest number of nodes of a network. Then, we complement this toolbox with algorithms for sensor placement so to also guarantee, when possible, observability of these nodes, thus allowing the implementation of feedback control strategies. Finally, an outlook on input selection strategies so to allow controlling a set of nodes of a network with reasonable energy is provided.

CHAPTER 1

Introduction

Abstract models of real world phenomena have been of paramount importance throughout the fields of science. The development of these mathematical representations has been mostly delegated to researchers of the physics community, as natural phenomena have been the main objects to be described. Some of these representations, such as Newton's three laws of motion, Maxwell's equations on electromagnetism, and Einstein's field equations have the character of theories due two their general validity. These have constituted the basis for the development of nearly an infinite number of laws and have constituted the anchor for countless real and numerical experiments.

In recent years, the enormous advances mankind has made in its comprehension of physical phenomena have brought more and more researchers to study real world systems such as power grids [10, 1], fish schools and other biological networks [53], financial markets [41], or social networks [57]. These systems cannot be described by separately modeling each of their components and ignoring their interactions as the latter play a crucial role in determining the overall system behavior. In fact, one could argue that a mathematical model of several of these systems cannot be formulated as some of their components to not obey to purely physical laws. Nevertheless, developing abstract representations able to capture some key aspects of their behavior can be critical [54, 11, 12, 8]. To do so, researchers have complemented methods of the physics community with tools from dynamical systems and graph theory, thus developing a new discipline, Networks Science, a paradigm for the interpretation and the description of the behavior of real world complex systems.

At first, the complex network paradigm has been mainly used as a tool for modeling the emergence of collective behavior in natural settings [2, 43, 47]. The laws that proved successful in capturing phenomena observed in nature have then inspired the design of control strategies able to reproduce these phenomena in artificial settings [58, 6, 65]. Prominent

examples are the numerous consensus protocols deployed for controlling the formation of fleets of autonomous vehicles [50, 52, 51, 9]. More recently, the use of the complex network paradigm has been extended to describe systems that do not exhibit emerging collective behaviors, but where modeling the interactions between the systems' components is critical in order to capture their main features. Skipping through the recent literature, we observe that financial systems, gene-regulatory networks, social networks, food webs and electronic circuits are frequently modeled as complex dynamical networks although they do not necessarily exhibit collective behaviors [31, 26, 8, 33, 57]. Consistently, from now on the term *Complex Network* will be used without specifying if it is referred to the real system or its mathematical abstraction, unless the contexts requires doing so.

Given the success that the complex network paradigm has had in describing the behavior of very diverse real world systems, it has been proposed as a testbed for control strategies aiming at affecting the behavior of these systems. From a theoretical perspective, the goal of being able to tame these complex networks has posed the following question: what are the conditions to be fulfilled in order to guarantee being able to arbitrarily affecting the behavior of a network? To answer this question, researchers have started by studying the following general problem: which nodes of a complex network must be directly controlled in order to be able to arbitrarily modify the behavior of the entire network? This problem has been widely studied in the recent literature and different metrics have been proposed for the optimal selection of the nodes to be directly controlled. Nevertheless, most of the recent literature has focused on gaining full control of the network behavior [37, 66, 61]. Here, we depart from the opposite perspective, as our point of view is that complex networks are perhaps too complex (!) to be fully controlled. This can be due to economic constraints limiting the number of nodes where input signals must be injected or to physical reasons, as the nodes that should be directly controlled in order to be able to affect the behavior of the whole network are inaccessible.

This shift of perspective from the ambition of completely controlling the behavior of complex networks to the more realistic goal of controlling only a fraction of the network nodes brings us to address two classes of problems. Firstly, we ask ourselves in which nodes shall we inject input signals so to maximize our ability to control the network behavior? Secondly, we face the problem of selecting the nodes where sensors should be placed so to be able to reconstruct the state of the nodes we are able to control.

Developing a toolbox of algorithms for the selection of the nodes where input signals must be injected so to maximize our ability to affect the network behavior allows us to break new ground in the analysis of the relation between the network structure and its readiness to

be made controllable. Our analyses ultimately lead us to define the network permeability to control signals, a measure of the propensity of a network to be made controllable. By analyzing the permeability of several real and model networks, we find that this index is strongly influenced by the networks structure. As a byproduct, we also find that both the nodes where input signals must be injected in order to maximize our ability to control a network and the nodes that are easily made controllable are characterized by structural signatures. Altogether, our findings provide the reader with a toolbox of algorithms for the selection of the nodes where input signals and sensors must be placed in complex dynamical networks together with a characterization of the structural properties that determine the network permeability and the ease with which the network nodes can be controlled.

1.1 Thesis outline

In Chapter 2 we introduce the general mathematical model of a complex dynamical network. Then, we introduce some notatation and mathematical preliminaries, mostly focusing on the graph-theoretic tools we will leverage to give our results. As we will study controllability of a specific class of complex networks, those that exhibit linear node dynamics, we intoduce the concept of controllability of linear systems and illustrate the theory of structural controllability. Finally, we illustrate how this theory can be leveraged to study controllability of complex dynamical networks.

After having given, in Chapter 2, all the theoretical background necessary to study controllability of complex networks, in Chapter 3, we introduce the concept of partial controllability of complex networks, which we define as the problem of selecting the nodes where input signals must be injected in order to maximize the number of nodes of the network that can be made controllable. Then, we give an algorithm able to solve this problem by first translating it into a graph optimization problem and then into an ILP. Finally, a discussion of the computational complexity of the ILP is given to end the chapter.

In Chapter 4, the tools developed in Chapter 3 are leveraged to uncover the ease with which complex networks can be made controllable regardless of the number of input signals deployed for the task. To measure the readiness with which a complex network can be made controllable, we introduce the network permeability to control signals, and we discover that this index is strongly tied to the network structure. We aslo find that the nodes where input signals must be injected in order to maximize our ability to control a network are characterized by structural signatures.

In Chapter 5, we exploit the results of the numerical analysis performed in 4 to develop heuristic driver node selection strategies with lower computational complexity than the strategy introduced in Chapter 3. In Chapter 6, we give an algorithm capable of solving the problem of placing a set of sensors in a subset of the network nodes in order to guarantee observability of the controllable nodes of a network. The aim of this Chapter is to complement the algorithms provided in Chapters 3 and 5 with sensor node selection strategies in order to allow deploying feedback control strategies for complex dynamical networks. Finally, in Chapter 7 Conclusions are drawn and an outlook is given on the current topics that are being investigated by the researchers working on controllability and control of complex dynamical networks.

The results given in Chapters 3 and 4 have been presented in ref. [40], while two papers presenting the results in Chapters 5 and 6 are under currently submission.

CHAPTER 2

Background

2.1 Complex networks

The complex network paradigm allows to model real world complex systems as an ensemble of dynamical systems, *the nodes*, interacting among each other according to an underlying topology. The general form of the equation describing the dynamics of the i-th of N network nodes is

$$\dot{x}_i = f_i(x_i) + \sum_{j \neq i} a_{ij} h_{ij}(x_i, x_j) \tag{2-1}$$

where x_i is the state of the i-th node of the network, $f_i(x_i)$ is the vector field describing its intrinsic dynamics, and $h_{ij}(x_i, x_j)$ is the function that defines the interaction between node i and node j. The binary coefficient a_{ij} indicates whether the dynamics of node i are, or are not, dependent on that of node j.

From a purely mathematical perspective, considering equation (2-1) for all the network nodes is sufficient to understand the network behavior, as is the case for all dynamical systems. Nevertheless directly approaching the dynamic equations of a network often proves unfeasible and not necessary. With some assumptions on the intrinsic node dynamics, several properties of complex networks can be studied by only taking into account the network topology and this, perhaps, is the main feature of the complex network paradigm. As this is the approach taken in this thesis, in the following section we introduce the graph theoretical tools necessary to cope with the topology of complex networks.

2.2 The structure of complex networks: algebraic graph theory

Rewriting eq. (2-1) for all the network nodes in compact form, we obtain the equation

$$\dot{x} = F(x) + AH(x), \tag{2-2}$$

where the matrix $A = \{a_{ij}\}$ is the adjacency matrix that defines the topology of the network, that is, a graph $\mathcal{G}(\mathcal{V}, \mathcal{P})$ where $\mathcal{V} = \{v_1, v_2, \dots v_N\}$ is the set of the N network nodes and $\mathcal{P} \subset \mathcal{V} \times \mathcal{V}$ is the set of network edges. In the graph $\mathcal{G}$ there is an edge p_{ij} connecting node v_j to node v_i if the corresponding binary element a_{ij} of the adjacency matrix A takes the value of 1. We can distinguish between two general categories of adjacency matrices which allow defining two general classes of graphs:

Definition 2.2.1. *A graph $\mathcal{G}$ is said to be undirected if its adjacency matrix is symmetric. In such case, the existence of the edge p_{ij} directly implies the existence of the edge p_{ji}.*

Definition 2.2.2. *A graph $\mathcal{G}$ is said to be directed (or a digraph) if its adjacency matrix is not symmetric.*

In this thesis, we will mainly focus on the general case of digraphs and, in some cases, show how some results simplify in the case of undirected network garphs. As we rely on structural controllability theory, we make use of the following definitions of elementary digraph structures [36]:

Definition 2.2.3. *A stem is an elementary path, i.e., a sequence of oriented edges $\{(p_{ij}), (p_{jk}), ..., (p_{lm})\}$ such that $i \neq m$. We will name the start node v_i a source, and the end node v_m a sink.*

Definition 2.2.4. *A cycle is an an elementary path that starts and ends in the same node.*

Definition 2.2.5. *We say that v_j is accessible from v_i if there exists a directed path from v_i to v_j and that in such a case v_i is in the upstream of v_j.*

Definition 2.2.6. *We say that a subgraph Γ of a graph $\mathcal{G}$ is stem-cycle disjoint if it is composed of an arbitrary number of stems and cycles that do not share any node nor edge.*

Moreover, we will make use of the following graph-theoretic definitions.

Definition 2.2.7. *A strongly connected component (SCC) of a graph $\mathcal{G}$, is a subgraph such that $\forall v_i, v_j \in SCC$ there exists a path from node v_i to node v_j.*

Definition 2.2.8. *A root strongly connected component (RSCC) of a graph $\mathcal{G}$ is an SCC r_i of $\mathcal{G}$ such that there are no edges entering a node of r_i that exit from a node that is not encompassed in r_i.*

Definition 2.2.9. *A Directed Acyclic Graph (DAG) is a graph that does not encompass cycles.*

Definition 2.2.10. *A digraph $\mathcal{G}(\mathcal{V}, \mathcal{P})$ contains a dilation iff there exists a set $T \subset \mathcal{V}$ that does not include source nodes, such that the number of elements in T is larger than the number of nodes having edges exiting them and entering the nodes in the set T. An example of a dilation is shown in Figure 2-1.*

Definition 2.2.11. *The indegree k_{in} of node v_i is equal to the number of edges entering node v_i.*

Definition 2.2.12. *The outdegree k_{out} of node v_i is equal to the number of edges exiting node v_i.*

Definition 2.2.13. *The sample indegree distribution of a digraph $\rho(k_{in})$ is a function that associates to each integer $k_{in} \in [0,\ \infty]$ the fraction of nodes having indegree equals to k_{in}.*

Definition 2.2.14. *The sample outdegree distribution of a digraph $\rho(k_{out})$ is a function that associates to each integer $k_{out} \in [0,\ \infty]$ the fraction of nodes having outdegree equals to k_{out}.*

Definition 2.2.15. *A set of edges $M \subset \mathcal{P}$ of a digraph is a matching if no two edges of M share a common starting or ending node. A matching is maximal if it is one of the possibly multiple matchings of a digraph of maximum cardinality.*

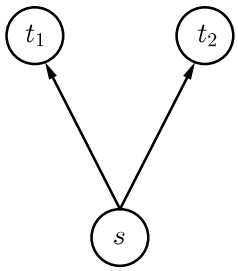

Figure 2-1: An example of a dilation, node t_1 and t_2 compose the set T while node s is the only node having an edge exiting it and entering the nodes of T.

Finally, as graph optimization problems often translate into Integer Linear Programs (ILPs), and as the characteristics of the matrices defining the constraints of these ILPs play a crucial role in determining their computational complexity, we give the following condition [7].

Lemma 2.2.1. *Let I be a $\{1,\ -1,\ 0\}$ value matrix in which each column contains at most two nonzero entries. Then, I is totally unimodular if its rows can be partitioned into two submatrices I_1 and I_2 such that:*

i. if two nonzero elements of a column have the same sign, they are either both encompassed in I_1 or both encompassed in I_2.

ii. if two nonzero elements of a column have opposite sign, then one is in I_1 and the other in I_2.

2.3 Networks of Linear Dynamical systems

The assumption of linearity of the node dynamics and of the coupling protocol between the network nodes allows to specify eq. (2-1) as

$$\dot{x}_i = f_{ii}x_i + \sum_{j \neq i} a_{ij}h_{ij}x_j \tag{2-3}$$

which, with a slight abuse of notation, allows to rewrite the dynamic equation of the network in (2-2) as

$$\dot{x} = Fx. \tag{2-4}$$

We can think of F as a *weighted* adjacency matrix, in which the diagonal elements f_{ii} capture both the existence of a self-loop and the intrinsic dynamics of the node v_i. Instead, the off-diagonal elements $f_{ij} := a_{ij}h_{ij}$ capture the existence of the edge p_{ij} and the associated coupling gain h_{ij}. If we consider F as a weighted adjacency matrix, we have to keep in mind that self-loops represent the intrinsic dynamics of the network nodes. If a node does not have a self-loop then we assume it behaves as a pure integrator.
While very few complex systems can be modeled through linear dynamics, these can capture the behavior of several systems about their equilibria. Moreover, when attempting to understand some general features of these systems, starting with simple dynamics so to focus on the role of their structure is often the best option. This has been the case with the topic of controllability of complex networks, as the seminal papers found in the literature [37, 38, 55] have focused on linear node dynamics.

2.4 Controllability of Linear Dynamical Systems

To study controllability of linear dynamical networks, we must first introduce the concept of controllability of linear dynamical systems. A linear dynamical system

$$\dot{x} = Fx + Bu \tag{2-5}$$

is said to be controllable if, through a suitable selection of the input signal u, it is possible to steer the state of the system from any initial condition $x(0)$ to any arbitrary final state x_f in finite time. If a system is not completely controllable, then it is possible to define the controllable subspace as the set of points from which the origin can be reached in finite time. Needless to say, if the system is completely controllable then the controllable subspace coincides with the state-space of the system. According to Kalman's criterion [27], the dimension of the controllable subspace is equal to the rank $\rho(K)$ of the so called controllability matrix

$$K = [B\ AB\ A^2B\ \ldots\ A^{N-1}B]. \tag{2-6}$$

The controllable subspace is the linear span of $\rho(K)$ linearly independent columns of the matrix K, and represents the subspace of the state space that is reachable from the origin through a suitable selection of the input signal u.

2.4.1 Structural Controllability of Linear Dynamical Systems

In 1974 Lin [36] noted that often the nonzero entries of the matrices F and B are only approximately known. Nevertheless, for single input systems he pointed out that as the set of all completely controllable pairs (F, b), is open and dense [32], if there exists a completely controllable pair $(\tilde{F}, \tilde{b})$, then there exists an infinite number of other pairs (F, b) with the same structure, that is, the same fixed (zero) entries, that are completely controllable. He thus defined the concept of structural controllability of a pair (F, b) as the existence of a pair $(\tilde{F}, \tilde{b})$ with the same structure of (F, b) that is completely controllable. Lin's results have then been generalized to the multi-input case by Shields and Boyd Pearson [56]. Formally, if a pair (F, B) is structurally controllable, then it is controllable for all values of the free (nonzero) entries of the pair except for a set with Lebesgue measure zero.

In 1980, Hosoe [16] generalized the concept of structural controllability to the case of non completely controllable systems, and thus to the controllable subspace. He noted that given a pair (F, B) with fixed structure, while the controllable subspace varies with the values of the free entries of the pair (F, B), its dimension remains stable except for a set of values of

the free entries with Lebesgue measure zero. This stable dimension is the so-called generic dimension of the controllable subspace.

A key feature of the structural controllability theory, and one that makes it extremely attractive for network scientists, is that the generic dimension of the controllable subspace can be computed by only inspecting the graph $\mathcal{G}(F, B)$ of the pair (F, B). Let us define the graph of the pair (F, B) as the graph $\mathcal{G}(F)$ [1] augmented with a number of nodes equals to the number of columns of B and thus representing the input signals. In $\mathcal{G}(F, B)$, if the ij-th entry of B is free, then an edge exits the i-th additional node and enters the j-th node of $\mathcal{G}(A_F)$. According to Hosoe, [16], the generic dimension of the controllable subspace is given by the number of edges of the largest stem-cycle disjoint subgraph of $\mathcal{G}(F, B)$ such that all stems originate in a node representing an input signal, and all nodes of the stem-cycle disjoint subgraph are accessible, in $\mathcal{G}(F, B)$, from at least a node representing an input signal. From this general condition, we can derive that a dynamical system is completely structurally controllable if the number of edges of the largest stem-cycle disjoint subgraph of $\mathcal{G}(F, B)$ is made of N edges, where N is the dimension of the system state.

2.5 Controllability of Complex Networks

By looking at eq. (2-4), we note that the dynamic equation of a complex network lacks an input matrix B. This is not accidental, as networks usually do not have predetermined driver nodes, that is, nodes where the input signals are injected. Hence, in the complex network paradigm, controllability must be seen as a property to be conferred through the selection of the driver nodes, rather than a structural property that the network may, or may not have. This is the perspective taken in the seminal paper by Liu et al. [37], where the authors claim that in the complex networks paradigm, controllability may be posed as the problem of selecting the minimal set of driver nodes that ensures the generic dimension of the controllable subspace be N, that is, the network be completely controllable. Formally, this means finding the matrix B with the minimum number of columns that ensures the network

$$\dot{x} = Fx + Bu \tag{2-7}$$

be structurally controllable.

In this new perspective in which controllability is a property to be endowed rather than verified, the need arises to complement the tools of structural controllability with methods

[1] where F must be considered a weighted adjacency matrix

and algorithms that allow optimizing some structural controllability metric through the selection of the driver nodes. In [37], the authors define the metric to be optimized as the number of input signals necessary to ensure a network be completely controllable and identify the tools needed to complement the structural controllability theory in the algorithms that allow finding the maximal matching of the graph $\mathcal{G}(F)$. Namely, they find that the minimal number of input signals required to ensure a network be completely controllable is equal to the number of unmatched nodes of the (possibly not unique) maximal matching of the graph $\mathcal{G}(F)$.

While in this thesis we view ref. [37] as a seminal paper due to the new perspectives it introduces, one limitation must be highlighted. Namely, the authors define the driver nodes as additional nodes representing input signals. To ensure complete controllability, we might need to inject each of these signals in more than one network node. Unfortuately, the maximal matching of a network only indicates one node where each signal must be injected. Hence, it does not provide complete information on where the control signals must be injected in order to ensure a network be completely controllable. In other words, relying on the maximal matching allows the authors to only identify the number of columns of the matrix B but only a subset of its free entries. Hence, the solution to the driver node selection problem provided in [37] does not define the structure of the matrix B fulfilling the structural controllability criterion.

Here, we take a different perspective as we make use of the following definition:

Definition 2.5.1. *A* driver node *is any node of the network in which an input signal is injected.*

To clarify the difference between the two definitions of a driver node, consider the network in Figure 2-2(a). The maximal matching of its graph is shown in Figure 2-2(b). Hence, according to the minimum input theorem provided in ref. [37], only one driver node (intended as an input signal) is required to gain full control of the network as the only unmatched node is node 4, the one highlighted in orange in Figure 2-2(c). Nevertheless the same signal, say u_1, injected in node 4 needs to be injected also in either node 1 or 2 as otherwise the state of these nodes would not be affected by the input signal, a necessary condition for these to be controllable. Unfortunately, this information is not provided by the maximal matching algorithm. Instead according to Definition 2.5.1 two driver nodes are required to gain full control of the network, for instance the two highlighted in red in Figure 2-2(d). The advantage is that finding the driver nodes as defined in Definition 2.5.1 unequivocally determines the structure of the matrix B. As we will show, considering Definition 2.5.1

causes an increase in the computational burden of the task of optimally selecting the driver nodes of a network

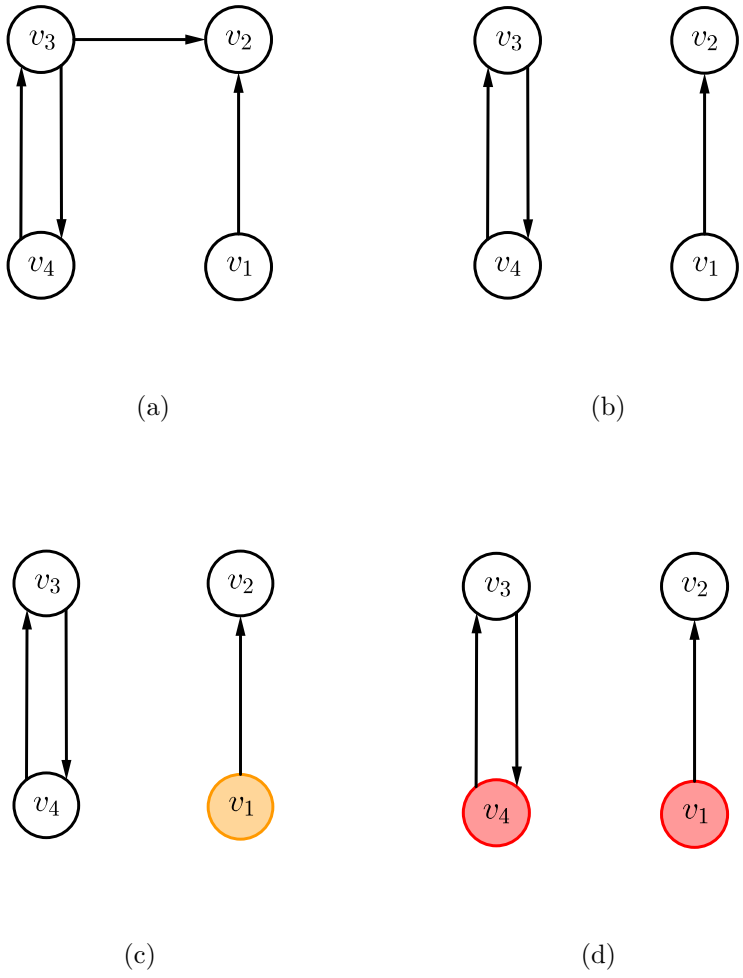

Figure 2-2: (a) The graph of a simple network (b) Its maximal matching. (c) The orange node is the only driver node selected by the maximal matching. (d) The red nodes are the driver nodes required to ensure complete controllability of this simple network according to definiton 2.5.1.

CHAPTER 3

Partial Controllability of Complex Networks

In Chapter 2, we have introduced controllability as a property that must be conferred to a network. Nevertheless, the perspective taken in this thesis is that ensuring a network be completely controllable is, more often than not, a chimera for two distinct reasons. Firstly, the scale of complex networks is often such that too many driver nodes would be required to fulfill such an ambitious requirement. To put things in perspective, consider that the complex networks paradigm has been proposed to model biological systems such as cellular networks [28]. Who could imagine to arbitrarily impose the state of all the cells of an organism? This same example brings us to our second point, complex systems have not been built to be controlled. The features of biological systems are mostly result of the evolution of species, the structure and functions of social networks vary with the number and characters of the people who enter these networks, and finally the structure of real world technological systems such as power grids grows and changes depending on the needs of the end users to be served. Hardly any of these complex systems are designed explicitly taking into account that the need can arise of controlling their behavior. Hence, it is reasonable to imagine that the access to nodes that can be crucial to guarantee complete controllability of the network might be precluded.

Motivated by these considerations, in this thesis we cope with the problem of developing driver node selection algorithms that allow maximizing the number of controllable nodes of a network while taking into account the economic and physical constraints that inevitably arise in applications. Before giving a formal statement of the main problem addressed in this thesis, let us define formally what we mean when we refer to the set of structurally controllable nodes of a network. As anticipated in Section 2.4.1, while the dimension of

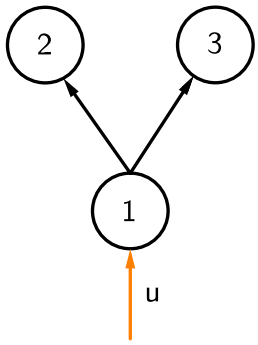

Figure 3-1: A very simple controlled network. The orange arrow indicates that the input u is injected in node 1 which is thus the only driver node.

the controllable subspace remains stable for all values of the free entries of the pair (F, B), the subspace itself varies. This is evident if we consider that the controllable subspace is obtained as the linear span of $\rho(K)$ linearly independent columns of the matrix K in eq. (2-6). As the free entries of the pair (F, B) vary, so do those of the matrix K. Hence, also the free entries of $\rho(K)$ linearly independent columns of K change along with their linear span, that is, the controllable subspace. Nevertheless, these free entries never assume the value of zero. Conversely, the fixed entries of the pair (F, B) do not vary, and thus neither do those of any $\rho(K)$ linearly independent columns of K. This essentially means that although the controllable subspace varies, the axes of the state-space along which it has non-zero components do not vary. These considerations imply that for any value of the free entries of the pair (F, B), there exists an input capable of arbitrarily imposing the state of the nodes of the largest stem-cycle disjoint subgraph of $\mathcal{G}(F, B)$ originating from the driver nodes. In other words, if a node is part of the largest stem-cycle disjoint subgraph of $\mathcal{G}(F, B)$, then we can arbitrarily impose its state. To make this point clearer, consider the simple network in Figure 3-1. The controllable subspace $\mathcal{K}$ is the linear span of the vectors $\mathbf{k_1} = [k_{11}\ 0\ 0]^T$ and $\mathbf{k_2} = [0\ k_{22}\ k_{32}]^T$, that is

$$\mathcal{K} = \{\lambda_1 \mathbf{k_1} + \lambda_2 \mathbf{k_2} \mid \lambda_1, \lambda_2 \in \mathbb{R}\} \tag{3-1}$$

and its projection onto the x_2, x_3 plane is the linear span of $\mathbf{k_2} = [0\ k_{22}\ k_{32}]^T$. In other words, from the origin, we can reach any point on the subspace $k_{32}x_2 = k_{22}x_3$ and thus we can either steer the state of node v_2 to an arbitrary value and let the state of node v_3 follow, or do the opposite. As shown in Figure 3-2, if the free entries of the pair (F, B) vary, also the controllable subspace does but its projection on the x_2, x_3 plane remains a straight line thus still allowing us to impose either the state of the node v_2 or of the node v_3. Consistently, we

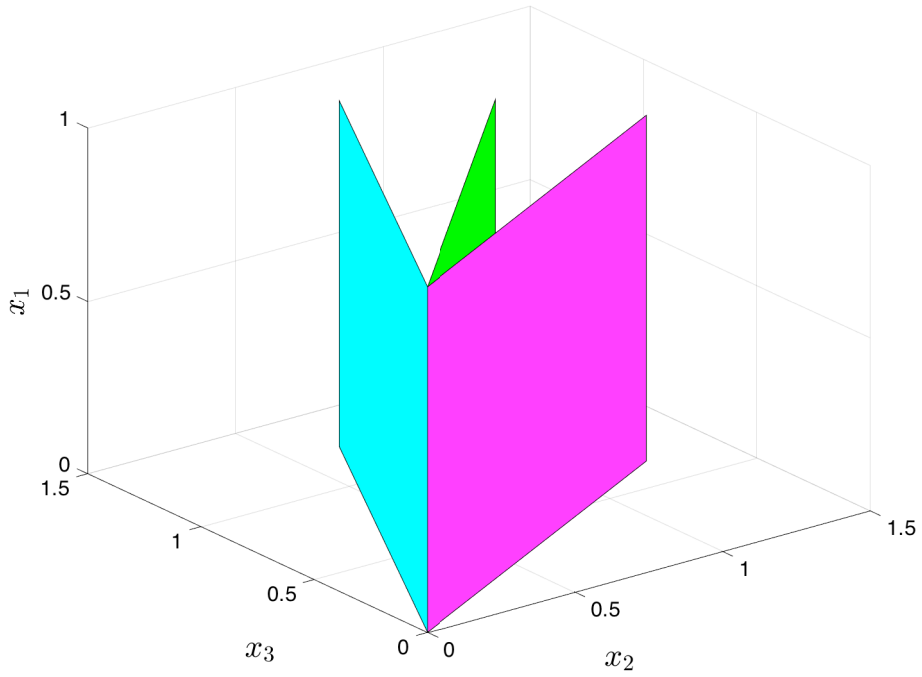

Figure 3-2: Plot of three different controllable subspaces corresponding to three different sets of values of the free entries of the pair (F, B) for the controlled network portrayed in Fig. **3-1**.

can choose as the largest stem-cycle disjoint subgraph either the stem p_{12} or the stem p_{13}, which means that we can consider controllable either v_1 and v_2 or v_1 and v_3.
Thanks to the aforementioned considerations, we can now give the following definition:

Definition 3.0.1. *The largest set of structurally controllable nodes of a network, say $\mathcal{C}$, is the set of nodes of the largest stem-cycle disjoint subgraph Γ of $\mathcal{G}(F, B)$ such that each stem originates from a node representing an input signal, and all the nodes of Γ are accessible from the drivers.*

Definition 3.0.1 constitutes the most general structural controllability condition that can be formulated for complex networks in it allows to determine the largest set of structurally controllable nodes[1] based on knowledge of the structure of the pair (F, B). As in this thesis we will rely on structural controllability theory, we will neglect the value of the free entries

[1] this set may not be unique

of the matrix F in equation (2-4). Hence, for simplicity, we will know on represent the dynamics of a linear dynamical network as

$$\dot{x} = Ax, \tag{3-2}$$

where each unit entry of the adjacency matrix A indicates the presence of a free entry in the matrix F in eq. (2-4), the exact value of which is unknown. We will resort to eq. (2-4) only if necessary and in this case we will explicitly refer to it.
In Chapter 2 we underlined that according to Liu et al. [37], in the complex network paradigm, controllability may be posed as the problem of selecting the minimal set of driver nodes that ensures the generic dimension of the controllable subspace be N. Following the same line of argument, but departing from the point of view that achieving complete structural controllability of a complex network is more often than not a chimera, in this thesis, we pose partial controllability of complex networks as the problem of selecting a set of nodes of fixed cardinality that maximizes the number of structurally controllable nodes. Moreover, to allow taking into account the constraints that inevitably arise in applications, we consider the case in which restrictions apply on the selection of the driver nodes. Specifically, we consider the case in which controllability is sought of a well-specified set of target nodes. This is the case, for instance, when attempting to design curative interventions for cancer, as one is typically interested in acting only on cells lying in carcinogenic and pre-carcinogenic state [68, 42]. Moreover, we take into account the case in which the selection of the driver nodes is restricted to a well-defined subset of the nodes of the network. A typical scenario of application of this condition is the design of curative interventions, when only some easily accessible proteins are designated as targets for drugs [29, 15, 44]. Finally, we allow considering the case in which the need arises of exerting these control actions without perturbing some nodes which are assigned to particularly important or vital functions. Some of these constraints have been recently considered in [13], where a heuristic strategy is proposed for selecting the driver nodes ensuring controllability of a set of target nodes. However, as stated in [13], a geometrical mapping of this problems is still lacking. In this thesis, we provide a toolbox of algorithms that allow tackling driver node selection problems for partial controllability of complex networks.

3.1 Problem Formulation

To give a formal statement of the main problem tackled in this thesis, we must first introduce the following notation.

- We denote by $\Omega \subset \mathcal{V}$ the set of admissible nodes of a network, that is, the set of nodes that can be selected as drivers;
- We denote by $\Omega_D \subset \Omega$ the set of nodes selected as drivers;
- We denote by $\Phi \subset \mathcal{V}$ the set of target nodes, that is, the nodes of a network that must be made structurally controllable;
- We denote by $\Psi \subset \mathcal{V}$ the set of untouchable nodes, that is, the nodes of a network that must not be perturbed by the control action;
- We denote by $\Xi_i \subset \mathcal{V}$ the set of nodes in the upstream of node v_i;
- Given a set Θ, we denote by $|\Theta|$ its cardinality, that is, the number of its elements.

We can now formally state the main problem addressed in this thesis:

$$\max_{\Omega_D} |\mathcal{C}| \tag{3-3}$$

s.t.

$$|\Omega_D| = M \tag{3-4}$$

$$\Omega_D \subset \Omega \tag{3-5}$$

$$\Phi \subset \mathcal{C} \tag{3-6}$$

$$\Big(\bigcup_{i|v_i \in \Psi} \Xi_i\Big) \cap \Omega_D = \emptyset. \tag{3-7}$$

Equations (3-3) and (3-4) translate the general problem of finding the set of driver nodes Ω_D of cardinality M that maximizes the number of controllable nodes. Moreover eqs. (3-5)-(3-7) formalize respectively the constraints that the driver nodes must be selected from the set of admissible nodes Ω, that the target nodes must be made controllable, and that the set of untouchable nodes Ψ must not be perturbed by the control action. Figure **3-3** illustrates a possible scenario of application of the stated problem.

The problem in eqs. (3-3)-(3-7) is stated in terms of sets of nodes as the toolbox of algorithms we provide to find its solution is mainly based on fulfilling graphical conditions. To conclude the transition presented in this chapter from the classical algebraic interpretation of controllability of linear systems to its graphical mapping leveraged in this thesis, we provide an algebraic interpretation of eqs. (3-3)-(3-4). Namely, we structure the input matrix B so to maximize the dimension of the controllable subspace with the constraint that B must have M columns each being a vector with only one free entry. If the entry b_{ij} of the matrix B is free, then node v_i has been selected as a driver node.

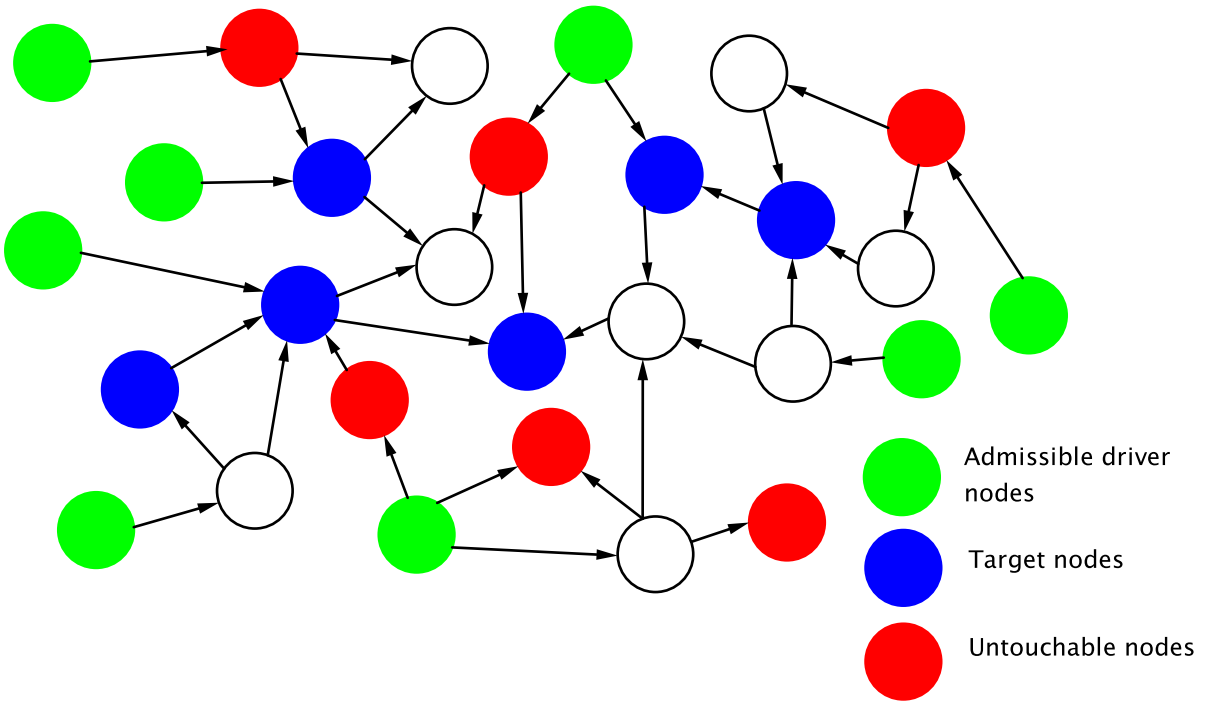

Figure 3-3: A possible scenario of application of the problem in equations (3-3)-(3-7). The green circles represent the nodes of the set Ω, the red cicles the nodes of Ψ, and the blue circles the nodes of Φ.

3.2 Problem Solution

To solve the problem in eqs. (3-3)-(3-7), the first step is that of deriving a graphical condition that ensures the selection of the set of driver nodes Ω_D is optimal. Indeed, the starting point must be Definition 3.0.1 which states that the generic dimension of the controlallable subspace is equal to the dimension of the largest stem-cycle disjoint subgraph Γ of $\mathcal{G}(A, B)$ such that all stems originate from the nodes representing the input signals, and all cycles are in the downstream of the nodes representing the input signals. Unfortunately, such condition is based on knowledge of the matrix B and thus on the set of driver nodes Ω_D which in our problem is obviously unknown. Hence, the graphical condition to be defined must determine the set Ω_D rather than depending on it.

Lemma 3.2.1. *The set of driver nodes Ω_D of fixed cardinality M that maximizes the number of structurally controllable nodes of a network $|\mathcal{C}|$ is given by the sources of the largest subgraph Γ_c of $\mathcal{G}(A)$ such that*

- *Γ_c is stem-cycle disjoint;*

- Γ_c *has* M *stems;*
- *each cycle of* Γ_c *is accessible, in* $\mathcal{G}(A)$ *from at least one source of the* M *stems.*

We choose as metric of the dimension of the subgraph Γ_c *the number of its nodes.*

In the condition defined in Lemma 3.2.1, we elect to change the metric of the dimension of a subgraph from the number of its edges to the number of its nodes. In definition 3.0.1, the chosen metric is the number of edges as the graph $\mathcal{G}(A, B)$ encompasses an additional set of nodes representing the input signals. Hence, measuring the dimension of the largest stem-cycle disjoint subgraph as the number of its nodes would lead to an overestimation of the dimension of the controllable subspace. On the other hand, as in stems and cycles each node has only one inbounding edge except for the sources of the stems which have none, measuring the dimension of the stem-cycle disjoint subgraph of $\mathcal{G}(A, B)$ as the number of its edges allows to ingore the nodes representing the input signals thus correctly evaluating the dimension of the controllable subspace. Here, Ω_D is to be determined and thus we must reason only on the graph of the network $\mathcal{G}(A)$. Hence, measuring the dimension of Γ_c as the number of its edges would lead to ignore the sources of the stems while chosing as a metric the number of its nodes allows correctly evaluating $|\mathcal{C}|$.
On the ground of Lemma 3.2.1, we can now give the algorithm developed to solve the problem in equations (3-3)-(3-7). Our algorithm is built in two phases. Firstly, starting from the graph $\mathcal{G}(A)$, we build an augmented graph $\mathcal{G}'$ that may be partitioned into disjoint cycles. Then, we formulate an ILP that performs an optimal cycle partition of $\mathcal{G}'$ by eliminating some of its edges. Removing, from the optimal cycle partition, the nodes and edges that are not part of the graph $\mathcal{G}$ we find the stem-cycle disjoint subgraphs Γ_c fulfills the condition expressed in Lemma 3.2.1 plus a set of isolated vertexes: the uncontrollable nodes. With this intuitive explanation in mind, we can now go through the steps of our algorithm.

Algorithm 1
Steps 1-7, construction of the graph $\mathcal{G}'$:

1. $\mathcal{G}'(\mathcal{V}', \mathcal{P}') = \mathcal{G}(\mathcal{V}, \mathcal{P})$.
2. Find the set $\Omega' = \{\Omega - \cup_{i|v_i \in \Psi} \Xi_i\} \subseteq \Omega$ of admissible nodes that do not have a vertex of Ψ in their downstream.
3. Add, to $\mathcal{G}'$, a set of M new nodes, say Θ, representing the M input signals to be injected in the network.

4. Remove, from $\mathcal{G}'$ all the nodes of Ψ and their upstream, along with all the associated edges.
5. Add $|\Theta| \times |\Omega'|$ new edges exiting each node of Θ and entering each node of Ω'.
6. Add $|\Theta| \times (|\mathcal{V}'| - |\Theta|)$ new edges exiting each node of $\mathcal{G}'$ that is also a node of $\mathcal{G}$ and entering each node of Θ.
7. Add a self loop one for each node of $\mathcal{G}'$ that is not a node of Θ nor of Φ.

Steps 8-11, finding the optimal cycle partition of $\mathcal{G}'$:

8 Associate a binary decision variable y_{ij} to each edge p'_{ij} of $\mathcal{G}'$.

9 Associate a unit weight w_{ij} to each decision variable y_{ij} that is either:
- associated with an edge p'_{ij} of $\mathcal{G}'$ that is also an edge of $\mathcal{G}$;
- associated with an edge p'_{ij} of $\mathcal{G}'$ that exits a node of Θ;

10 Associate zero weight w'_{ij} to all the other decision variables y_{ij}:

11 Solve the following Integer Linear Program:

$$\max_{y} \quad \sum_{i} \sum_{j} w'_{ij} y_{ij} \tag{3-8}$$

subject to

$$y_{ij} \in \{0,1\} \quad \forall i,j | p'_{ij} \in \mathcal{P}' \tag{3-9}$$

$$\sum_{j} y_{ij} = 1 \quad \forall i = 1, ..., N+M \tag{3-10}$$

$$\sum_{i} y_{ij} = 1 \quad \forall j = 1, ..., N+M \tag{3-11}$$

$$\sum_{l \in \Xi_i} \sum_{j \in \Theta} y_{lj} \geq \sum_{j} w'_{ij} y_{ij} \quad \forall i = 1, ..., N+M \tag{3-12}$$

The proposed algorithm first builds an augmented graph $\mathcal{G}'$ in which the M input signals to be injected in the network are represented as additional nodes belonging to a set Θ. The edges exiting the nodes of Θ point only to the nodes of Ω', so to restrict the selection of the drivers to the admissible nodes that do not have any untouchable node in their downstream. Instead, the added edges that point to the nodes of Θ (step 5) allow reducing the M stems originating from the additional nodes to cycles. Finally, in order to make sure there exists a cycle partition of $\mathcal{G}'$, self loops are added to each node of $\mathcal{G}'$ that is not a target node.

Now, the problem in eqs. (3-3)-(3-7) can be translated into a problem on the graph $\mathcal{G}'$. We must *select, among all the cycle partitions of $\mathcal{G}'$, the one that encompasses the maximum number of edges p'_{ij} that are also edges of $\mathcal{G}$ satisfying the following constraint: the nodes in cycles encompassing edges p'_{ij} that are also edges of $\mathcal{G}$ must be accessible, in $\mathcal{G}$, from the nodes selected as drivers.*

This problem translates into the Integer Linear Program (ILP) in eqs. (3-8)-(3-12). Specifically, a binary decision variable y_{ij} is associated with each edge p'_{ij} of the graph $\mathcal{G}'$; if $y_{ij} = 1$, then the corresponding edge p'_{ij} will be part of the cycle partition. The product $w'_{ij}y_{ij}$ will return a unit cost either when the selected edge of $\mathcal{G}'$ is also an edge of $\mathcal{G}$ or if the edge exits a node of Θ. As, in the cycle partition, the edges exiting the nodes of Θ enter the nodes that are selected as drivers, these are constrained to be M as prescribed by eq. (3-10). Hence, eq. (3-8) translates the goal of maximizing the number of edges of $\mathcal{G}'$ that are also edges of $\mathcal{G}$. Moreover, as the nodes of the cycle partition with an inbounding edge of unit weight compose the set $\mathcal{C}$, and as all edges with unit weight only enter nodes of $\mathcal{G}'$ that are also nodes of $\mathcal{G}$, eq. (3-8) represents the maximal achievable cardinality of the set of controllable nodes thanks to Lemma 3.2.1. Every other selected edge will not contribute to the objective function and is to be viewed as a slack variable as it is only needed to form a cycle.

The role of the constraints of the ILP is that of ensuring the solution fulfills the requirements of the problem in eqs. (3-3)-(3-7). Namely, eqs. (3-10) and (3-11) guarantee that the optimal solution be a cycle partition of $\mathcal{G}'$ by forcing each one of its vertices to have exactly one entering and one outgoing edge, while eq. (3-12) forces all the nodes of $\mathcal{C}$ to be accessible from at least one of the driver nodes. This is done by ensuring that if a node has an entering edge with unit weight then there is at least a node in its upstream that has an edge with unit weight entering it that exits from a node of Θ. Note that the constraints on the target, admissible, and untouchable nodes in eqs. (3-5)-(3-7) are fulfilled through the construction of the graph $\mathcal{G}'$. Namely, thanks to steps 2 and 5, all the nodes that are in the upstream of the untouchable nodes do not have an inbounding edge that exits the nodes of Θ, thus ensuring that the nodes of the set Ψ are not perturbed by control signals. Morover, thanks to step 7, the target nodes do not have inbounding edges with zero wight and thus must be included in the set $\mathcal{C}$. Finally, thanks to step 5, only the admissible nodes can be selected as drivers.

An example of application of our method when $M = 1$ is shown in figure 3-4; the orange node in figure 3-4b) represents the input signal, while the orange and blue edges are those added to enable the formation of a cycle partition. The nodes with inbounding black or orange edges are those encompassed in $\mathcal{C}$.

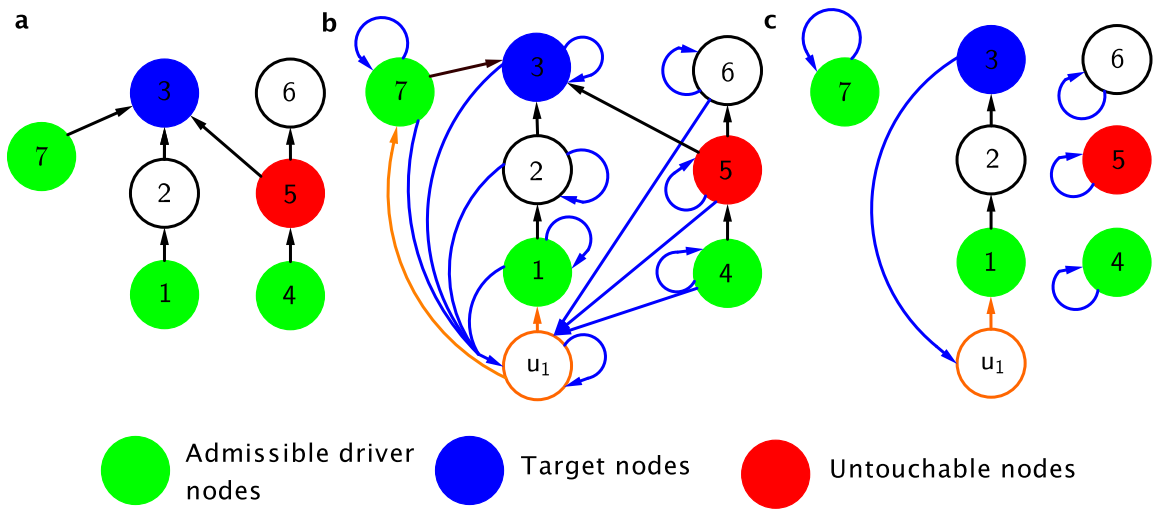

Figure 3-4: An example of application of our method

The developed algorithm us to deal, as particular cases, with the following two relevant problems.

a. Finding the node with maximum centrality When (i) the set Ω coincides with the entire set of vertices of $\mathcal{G}$ and (ii) the sets Φ and Ψ are empty, specifying our algorithm for $M = 1$ allows us to determine the node with maximum control centrality [38].

b. Finding the largest set of controllable nodes given the set of driver nodes (Hosoe's theorem) When (i) the set Ω_{D} is given and (ii) the sets Φ and Ψ are empty, the proposed algorithm allows us to determine the set of controllable nodes, given the set of driver nodes. Note that in this scenario, our algorithm reduces to Poljak's [49] method as the set Ω_{D} is given and no driver node has to be selected.

Feasibility of the proposed method We rely on the implicit assumption that our method is applied to a well formulated problem, *i.e.,* a problem that admits a solution. However, this would not be the case, for instance, if an untouchable node were in the downstream of a target node, as for the latter to be controllable, the former must be influenced. We remark that the feasibility issues are not related to our method but to the problem itself. Hence, if our method does not output a solution, then a solution to the problem does not exist in the structural controllability framework.

As anticipated, the viewpoint taken in this thesis is that gaining full control of complex networks is, more often than not, a chimera leading us to shift our perspective towards controlling just a fraction of the network nodes. Equations (3-3)-(3-7) translate this conceptual idea in the problem of finding the set of driver nodes Ω_D of fixed cardinality that maximizes the cardinality $|\mathcal{C}|$ of the set of structurally controllable nodes of a network. In what follows,

we propose a formulation that translates the same conceptual idea of controlling only a fraction of the network nodes into a different optimization problem, namely that of finding the set of driver nodes of minimum cardinality that allows achieving structural controllability of a well defined set of target nodes Φ while fulfilling the constraints on admissible and untouchable nodes:

$$\begin{aligned} &\min_{\Omega_D \subset \Omega} |\Omega_D| \\ &\text{subject to} \\ &\Phi \subset \mathcal{C} \\ &\cup_{i \in \Psi} (\Xi_i) \cap \Omega_D = \emptyset. \end{aligned} \tag{3-13}$$

Coping with this problem requires only minor tweaks to the algorithm described above. As the number of driver nodes is now to be determined and is bounded by the cardinality of Ω', in step 3 we will have that $|\Theta| = |\Omega'|$ as $|\Omega'|$ new nodes representing input signals must be added to the graph $\mathcal{G}'$. Moreover, as it is possible that less than $|\Omega'|$ driver nodes are required to ensure structural controllability of the set Φ, in step 7, a self loop must be added to each of the nodes of Θ. Furthermore, the objective function of the ILP (Eq. (3-8)) must now read

$$\min_{y_{ij}|v_j \in \Theta} \sum_{j|v_j \in \Theta} \sum_{i} w'_{ij} y_{ij}. \tag{3-14}$$

Thus, in this case, a cycle partition is sought that minimizes the number of driver nodes necessary to fulfill the requirement on the target and untouchable nodes. The vertices representing input signals that are not injected in the network form cycles of their own thanks to the additional self loops. Again, our algorithm assumes that the problem is well formulated, i.e., that it admits a solution in the structural controllability framework. Again this general formulation allows us to cope, as particular cases, with two prominent problems.

a. Finding the MDS of a network If (i) the sets Ω and Φ coincide with the entire set of vertices and (ii) Ψ is empty, solving the problem in equation (3-13) corresponds to finding the set of driver nodes of minimum cardinality that ensure complete controllability of a network [37].

b. Target Controllability When (i) Ω coincides with the entire set of vertices, (ii) Ψ is empty, and (iii) Φ is a well defined subset of nodes, solving solving the problem in equation (3-13) allows to find an optimal solution to the problem for which a heuristic strategy is proposed in [13].

3.3 Computational Considerations

Research on complex networks has always been closely tied to computational issues for two distinct reasons. First of all, complex networks are large scale systems and for this simple reason any tool or method easily used for low-dimensional dynamical systems might turn out requiring too much computational power when applied to complex networks. For instance, as highlighted by Steven Strogatz in his distinguished review [59], only of late *the availability of powerful computers has made it feasible to probe* the structure of complex networks. Second of all, most choice problems that translate into graph optimization problems are solved by performing a second translation into ILPs. Notable examples are the shortest path problem, scheduling problems, or the well-known traveling salesman problem. Driver node selection problems for complex networks make no exception to this general rule as, leveraging the structural controllability theory, they can be translated into graph optimization problems. As shown in the previous section, the latter can again be translated into ILPs thanks to the general algorithm proposed in this thesis. Unfortunately, ILPs are, in general, Non-deterministic Polynomial time hard (NP-hard). Without entering into the details of computational complexity theory (which is beyond the scope of this thesis), this means that there is no guarantee these problems can be solved in polynomial time, although there is no proof of the opposite as well.

The fact that ILPs are, in general, NP-hard does not mean that any problem that admits a translation into an ILP is actually NP-hard. For instance, the shortest path problem is best formulated as an ILP but can be solved performing a relaxation to a Linear Program (LP), that is, ignoring the integer constraint on the decision variables, which makes the problem solvable in (weakly) polynomial time. Moreover, several problems that naturally translate into ILPs admit ad-hoc algorithms capable of finding the optimal solution. In fact, nobody would ever solve a shortest path problem by solving the associated LP as several much faster algorithms have been developed to find the optimal solution.

From these considerations, the question of if driver node selection problems can be solved in polynomial time naturally arises. Let us start providing an answer by discussing the case of finding the minimal set of driver nodes (MDS) necessary to ensure complete structural controllability of a complex network, that is, the problem dealt with in ref [37]. If relying on definition 2.5.1, finding the MDS of a network ultimately reduces to solving an ILP the objective function of which is defined in equation (3-14) subject to the constraints in equations (3-9)-(3-12). The question becomes: is it possible to relax the ILP to an LP which, in general, can be solved in (weakly) polynomial time and still obtain an integer

solution? The algebraic condition that ensures the solution of an LP be integer is that the matrix defined by its constraints is totally unimodular and that the constant terms are all integers. In this case, the polytope defined by the constraints has vertices with only integer coordinates. As it is well known that the solution of a Linear Program lies on a vertex of the polytope defined by its constraints, it follows that if the matrix defined by the constraints of an ILP is totally unimodular, and if the constant terms are all integers, then the solution of the LP relaxation of an ILP is also the solution of the ILP. By inspecting equations (3-10)-(3-12) we can immediately note that the constant terms of our constraints are all integers. Moreover, the matrix defined by the equality constraints in eqs. (3-10) and (3-11) is totally unimodular as it verifies the sufficient condition given in Lemma 2.2.1. Namely, we note that all the free entries of the matrix defined in equations (3-10) and (3-11) take the value of 1, and thus, performing the decomposition in two blocks I_1 and I_2 proposed in Lemma 2.2.1, we have that one of the two, say I_1, is empty while the other, say I_2, encompasses all the matrix. Moreover, we note that each each column of the matrix contains only two non-zero entries. This as each decision variable y_{ij} represents an edge p'_{ij} of the graph $\mathcal{G}'$, and thus it is encompassed only once in the constraint in equation (3-10) which ensures that in the optimal cycle node v_j has only one edge exiting it and once in the constraint in equation (3-11) which ensures that in the optimal cycle partition node v_i has only one edge exiting it. As the constraints in equations (3-10) and (3-11) force the solution of the ILP be a cycle partition of the graph $\mathcal{G}'$, this means that finding a cycle partition of a graph is a problem that can be solved in polynomial time. Going back to our problem, unfortunately equation (3-17) spoils the total unimodularity of the constraint matrix of our ILP. Thus, adopting definition 2.5.1 we obtain that finding the MDS of a network is a problem that cannot be solved in polynomial time. As underlined in section 3.2, the constraint in eq. (3-17) ensures each node of $\mathcal{C}$ be accessible from a driver node in the graph $\mathcal{G}$. Here, we add that considering this constraint is what differentiates definition 2.5.1 from that given by Liu et al. in ref. [37]. This as if a cycle is not accessible from at least a node where a control signal is injected, then a control signal must be injected in an arbitrary node of the inaccessible cycle to guarantee controllability of all of its nodes. Nevertheless, as this control signal can be the same as that injected in any other node of the network, the number of distinct control signals to be injected in the network in order to ensure the latter be completely structurally controllable does not change. Hence, adopting the definition of a driver node given in [37] ensures the problem of finding the MDS of a network is solvable in polynomial time. This comes at the price of not being able to determine the complete structure of the matrix B. Moreover, the perspective taken in this thesis is that limitations are often imposed on the number of

nodes in which a signal is injected, rather than on the number of distinct signals deployed for the control action. Finally, from an energetic standpoint, injecting the same signal into two different nodes may be inefficient as the same control action is used to achieve a larger number of objectives. To better understand this point consider the problem of steering the linear dynamical system

$$\dot{\mathbf{x}} = A\mathbf{x} + B\mathbf{u} \tag{3-15}$$

where $\mathbf{u}(t) = [u_1(t)\ u_2(t)]^T$, from an initial state $\mathbf{x}(0)$ to a desired final state $\mathbf{x}(t_1)$. In order to minimize the energy required to achieve the control goal, $\mathbf{u(t)}$ is chosen as the solution of the following optimization problem:

$$\min_{\mathbf{u(t)}} J := \int_0^{t_1} \mathbf{u(t)}^T \mathbf{u(t)} dt, \tag{3-16}$$

As imposing $u_1(t) = u_2(t)$ represents a constraint for the optimization problem in (3-16), bounding two signals to be identical can only yield an increase in the optimal J.
To provide a general answer to the question of if the driver nodes selection strategy proposed in this thesis is NP-hard we point out that solving the problem in equations (3-3)-(3-7) requires solving the ILP in equations (3-8)-(3-12). Again equation (3-12) ensures the constraint matrix is not totally unimodular and thus also finding the set of driver nodes of fixed cardinality so to maximize the number of controllable nodes of a network is NP-hard.
Given the NP-hard nature of the ILP in equations (3-8)-(3-12) the following question naturally arises: does it prove unsolvable for large networks? Absolutely not. As testified by the numerical results reported in the next chapter, we have solved millions of instances of the ILP in eqs. (3-8)-(3-12) for networks of up to 10^4 nodes and we have never been forced to resort to heuristic strategies. Instead, we focused on finding the strongest possible formulation of our problem. To obtain this strengthened formulation, in the construction of $\mathcal{G}'$ we only add one additional node representing all the input signals (step 3 of our algorithm). This node, denoted as $N+1$, now plays the role of all the nodes of Θ and is connected to all of the other N nodes of $\mathcal{G}'$ with both inbounding and outgoing edges. Node $N+1$ has the ability to *close* all of the M cycles that include a driver node. Coherently, the equality

constraints in Eqs. (3-10) and (3-11) are changed to

$$\sum_j y_{ij} = 1 \quad \forall i = 1, ..., N \tag{3-17}$$

$$\sum_i y_{ij} = 1 \quad \forall j = 1, ..., N \tag{3-18}$$

$$\sum_j y_{N+1,j} = M \tag{3-19}$$

$$\sum_i y_{i,N+1} = M. \tag{3-20}$$

The advantage of this new formulation is that it considerably reduces both the number of variables and the number of constraints. Namely, the number of variables that this new formulation allows to remove is $|\mathcal{V}'| \times (M-1) + |\Omega'| \times (M-1)$ as instead of adding M new nodes representing the input signals which must then be connected with outgoing edges to all the nodes of Ω' and with inbounding edges with all the nodes of the graph $\mathcal{G}'$, we only add one. Moreover, the number of constraints is reduced by $2 \times (M-1)$ as again only one node is added to represent the M input signals and thus only two additional constraints must be considered to force the edges exiting and entering this node be M instead of $2M$ additional constraints ensuring each node of Θ has one entering and one exiting edge. Note that the proposed strengthened formulation is sill characterized by the total unimodularity of the matrix defined by the constraints (3-17)-(3-20). This as equation (3-17) is the same as equation (3-10) except for it only holds for $j = 1, ..., N$ instead of $j = 1, ..., N+M$. Moreover, the same reasoning applies to the relationship between equations (3-18) and (3-18). Finally, as equation (3-19) is the same as $N+1$-th constraint defined by equation (3-17) only with a constant term that is still integer but equals to M, and the same reasoning applies to the relationship between equation (3-20) and the $N+1$-th constraint defined by equation (3-18), the condition in Lemma 2.2.1 is still verified.

Although all numerical results reported in this thesis have been obtained using the strengthened fomrulation in eqs. (3-17)-(3-20) but only relying on standard ILP solvers such as those implemented in Matlab and Gurobi, for completeness, we have developed an ad-hoc algorithm for the solution of our ILP based on the property that the equality constraint matrix is totally unimodular. As we will show in what follows, this structural property can be exploited to strongly reduce the computational complexity of the ILP. The idea behind our strategy is that of complementing the general *Branch and Cut* techniques used to solve ILPs with ad hoc *bounding* and *cutting* procedures able to exploit the special structure of our problem.

Bounding: estimation of an upper bound for $|\mathcal{C}|$. An approximation of $|\mathcal{C}|$ from above can

be obtained from a relaxed version of our problem.

Relaxation A: a first relaxation can be obtained, as usual, by removing the integrity constraints on the decision variables y_{ij} thus transforming the ILP into an LP. Note that as the equality constraint matrix is totally unimodular often this relaxation will yield an integer solution allowing the ILP to stop at the root LP solution. This as several vertexes of the polytope defined by the entire set of constraints in equations (3-12) and (3-17)-(3-20) will be also vertices of the totally unimodular matrix defined by the constraints in (3-17)-(3-20), which we know are integer.

Relaxation B: a second strategy is that of relaxing constraint (3-12). In this case the problem becomes that of finding the cycle partition of $\mathcal{G}'$ that maximizes our objective function. As the equality constraint matrix is totally unimodular, also this problem reduces to a LP. Obviously, in bounding from above the objective function of problem (3-8) - (3-12) the minimum between the two estimates can be selected.

Bounding: estimation of a lower bound for $|\mathcal{C}|$. An approximation from below of the number of controllable nodes can be obtained from Relaxation B. Indeed, the solution of the relaxed problem offers a cycle covering of the graph $\mathcal{G}'$ for which not necessarily each cycle is accessible from the drivers. By subtracting the number of nodes located in inaccessible cycles to the objective function we get the approximation required.

Ad hoc Cutting procedures The branching phase in ILP solution methods is always complemented with a *cutting* procedure. Cuts are additional constraints added to the ILP that allow strengthening the formulation without eliminating feasible solutions. In our case, if the upper bound resulting from Relaxation A is tighter, then standard cuts (Gomory, Strong, etc.) and binary branching strategies are to be applied (although always taking into account the availability of a lower bound). On the other hand, if the upper bound obtained by relaxing the constraints in (3-12) is tighter, then two *ad hoc* cutting strategies can be deployed *which exploit* the structure of our problem. Both consist in applying recursively some constraints.

Strategy 1: The first ad hoc cutting strategy consists of the following steps:

1. Relax the constraints in Eq. (3-12) and solve the LP relaxation of the resulting ILP. The solution will be integer as the equality constraint matrix is totally unimodular. This yields a set of driver nodes Ω_{D}^1 and a set of controllable nodes $\mathcal{C}^1$;

2. If each node of $\mathcal{C}^1$ is accessible from at least one node of Ω_{D}^1 then the optimal solution is found;

3. Otherwise, $|\mathcal{C}^1|$ is an upper bound for the optimal value $|\mathcal{C}^*|$;

4. Remove the inaccessible nodes from $\mathcal{C}^1$ to obtain a lower bound for $|\mathcal{C}^*|$ along with the largest set of controllable nodes from the set of drivers Ω_{D}^1;

5. Apply the inequality constraint

$$\sum_{l \in \Omega_{\mathrm{D}}^1} y_{l,N+1} \leq M - 1 \tag{3-21}$$

to exclude the set Ω_{D}^1 from the possible sets of drivers and solve the LP relaxation of the new ILP.;

6. If the solution is integer but unfeasible as some cycles are inaccessible, two new bounds can be computed as in steps 3 and 4. Take the tightest among the available bounds and repeat steps 5 and 6 until either an integer feasible solution or a non-integer feasible solution is found;

7. If an integer feasible solution is found, then the optimal solution is the best one between such solution and the current lower bound;

8. If on the other hand a non-integer solution is found, then this is the tightest possible upper bound. Now, the standard cuts and branching strategies must be applied (taking into account the availability of upper and lower bounds to enhance the pruning procedure).

Strategy 2: The first four steps of the second *ad hoc* cutting strategy coincide with the first four steps of *Strategy 1*. These must be complemented by the following steps;

5. Amongst the inequality constraints in (3-12) apply only those violated by the solution obtained at step 1;

6. If the solution is integer but unfeasible, as some cycles are inaccessible, two new bounds can be computed as in steps 3 and 4. Take the tightest among the available bounds and repeat steps 5 and 6 until either an integer feasible solution or a non-integer feasible solution is found;

7. If the solution is integer and feasible, then it is optimal;

8. If the solution is non-integer and feasible, then this is the tightest possible upper bound. Now, the standard cuts and branching strategies must be applied (taking into account the availability of upper and lower bounds to enhance the pruning procedure).

The idea behind both cutting strategies is that the sequence of upper and lower bounds obtained by exploiting the total unimodularity of the equality constraint matrix can drive the search toward the true solution. While these strategies have been designed to complement standard branch and cut algorithms in order to find the optimal solution, if the search is stopped before the solution is found (because it exceeds the maximum time, for instance) an interval of uncertainty on the number of controllable nodes is obtained along with (at least) a feasible solution. Hence, the two defined strategies can also be viewed as simple heuristics. In the next chapter, we will discuss some more sophisticated heuristics which have been developed in order to cope with driver node selection problems in huge complex networks (networks with over 10^5 nodes).

CHAPTER 4

Structural Permeability of Complex Networks to Control Signals

In Chapter 2 we have defined controllability of a linear dynamical system as a structural property of the pair (F, B) in equation (2-5). Moreover, we have underlined that in the complex network paradigm we have to view controllability as a property that must be conferred to a network as, more often than not, the driver nodes are not given a priori but must be selected. Still, as shown by Liu et al. in ref [37] the network structure may facilitate, or hinder, our ability to make a network structurally controllable. Namely, the authors link the propensity of the network structure to be made completely controllable to its degree distribution and, relying on the cavity method [45, 67], they derive a set of self-consistent equations able to predict the number of driver nodes required to achieve complete controllability of a network based on the degree distribution of its topology. By applying the cavity method to several real and model network topologies, they find that sparse heterogeneous networks are harder to be made completely controllable than dense homogeneous networks. The authors also provide numerical evidence confirming their analytic predictions.

Spurred by these results, several researchers have studied the relation between the network structure and its propensity to be made completely structurally controllable. For instance, Ruths and Ruths [55] have studied the network motifs that affect controllability, while Liu et al. [38] the relation between the network degree distribution and its maximum control centrality, that is, the dimension of the largest set of controllable nodes achievable by leveraging only one driver node. Then, driven by the same idea of linking our ability to control a network to its structure, researchers have crossed the boundary of structural controllability. For instance, Nepusz and Vicsek [46] have explored the option of introducing a dynamical process on the network edges and found that the controllability properties of this process

may be substantially different from those of simple node dynamics. While these references only represent a small sample of the bulk of work studying the relation between the structure and function of complex networks and their propensity to be made completely controllable, we still lack indications on how the network structure affects our ability to control part of a network. In fact, as up to date we lack optimal driver node selection algorithms aiming at guaranteeing controllability of the largest set of the network nodes, we are unable to even measure the readiness of a network to be made controllable if not in the sense of complete structural controllability. Having filled the methodological void thanks to the toolbox of algorithms presented in chapter 3 we know face the task of defining a measure of the readiness of a network to be made controllable regardless of the number of driver nodes deployed for the task.

We start by pointing out that solving the maximization problem in eqs. (3-3)-(3-7) for each value of M in the interval of integers $[1, N]$ without restrictions on the admissible, target, and untouchable nodes allows us to obtain the sequence of sets of optimal driver node $\Omega_{\mathrm{D}}(M)$ and the corresponding dimension of the maximal set of controlallable nodes with M drivers $|\mathcal{C}(M)|$. Figure 4-1 portrays the sequence $|\mathcal{C}(M)|$ for the Budding Yeast Protein Structure network (blue)[4] and the SciNet citation network (red). We note that providing an answer to the question of which one has a greater readiness to be made controllable is nontrivial, as apparently it varies depending on the number of driver nodes M. Namely, in Fig. 4-1 we observe that for small values of M the blue curve lies above the red one, while the opposite is observed for $M > 0.1N$.

To measure the readiness of a network to be controllable, we define the network permeability to control signals $\mu \in [0, 1]$, which, in the thermodynamic limit, can be computed as

$$\mu = \frac{\int_0^N (|\mathcal{C}(M)| - M)dM}{\int_0^N (N - M)dM} = \frac{2}{N^2} \int_0^N (|\mathcal{C}(M)| - M)dM \tag{4-1}$$

For a given network, μ is the difference between the area under the curve $|\mathcal{C}(M)|$, and the same area relative to an ensemble of N disconnected nodes for which $|\mathcal{C}(M)| = M,\ M = 1, ..., N$. This quantity is then divided by the area under the curve $|\mathcal{C}(M)| = N,\ M = 1, ..., N$ so that μ takes the value of 1 for networks that are completely controllable by means of one driver node and the value of 0 for ensembles of disconnected nodes. The integral operator allows μ to take into account the dimension of the maximal set of controllable nodes for all values of M. We emphasize that while controllability is a property of a network together with the selected driver nodes, μ is only related to the network itself. Hence, the permeability allows us to measure for the first time the propensity of a network to be made controllable,

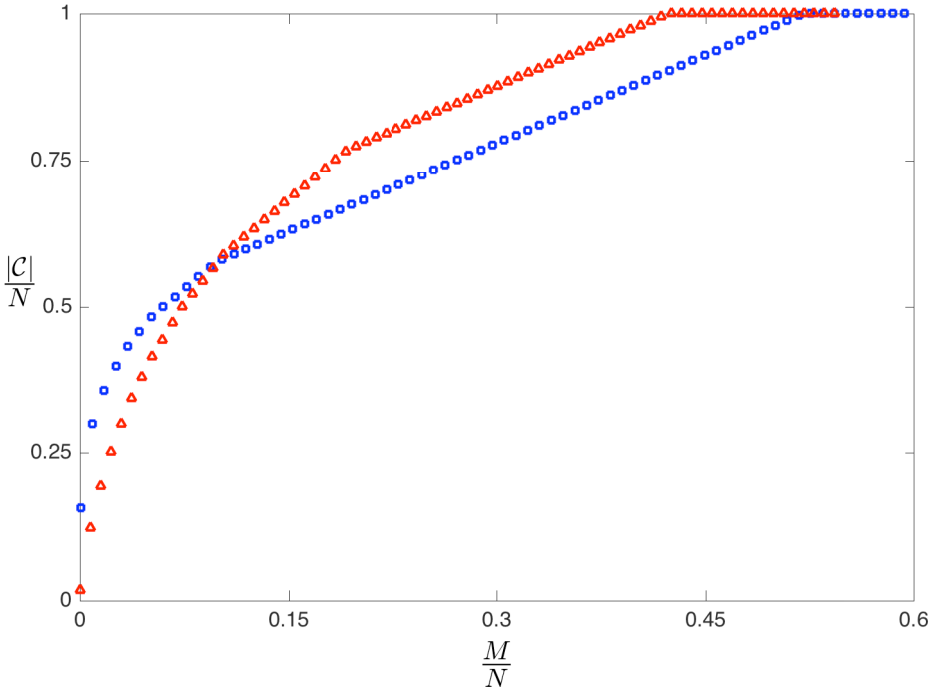

Figure 4-1: Plot of the sequence $|\mathcal{C}(M)|$ for the Budding Yeast Protein Structure network (blue) and the SciNet citation network (red). Both $|\mathcal{C}(M)|$ and M are normalized by dividing them by number of nodes of the two networks to allow comparing the results on the same scale.

that is, the extent to which the network structure facilitates the diffusion of the control signals.

4.1 Permeability analysis of real network topologies

Leveraging the algorithm defined in chapter 3, we have analyzed a number of real and artificial networks in order to shed light on the relation between their structure and their permeability. As our driver node selection algorithm reduces to extracting cycles from a graph, one could expect that networks with average high degree $\langle k \rangle$ are highly permeable. Surprisingly, as shown in figure 4-2 we observed that real networks with similar $\langle k \rangle$ can exhibit large variability in their permeability. For instance, we note that the only transcription network topology analyzed exhibits a much smaller permeability with respect to the set of metabolic network topologies despite having similar average degree. Coherently, we find a

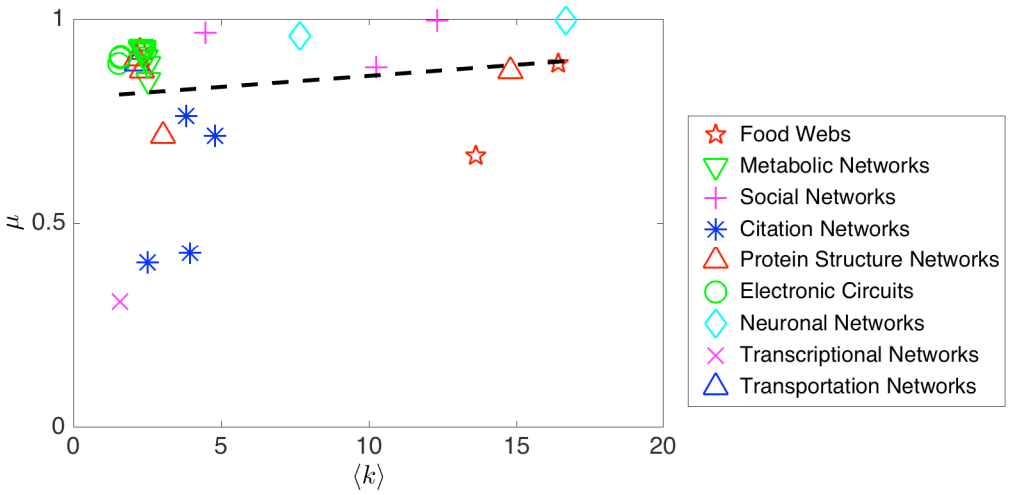

Figure 4-2: Plot of the network permeability μ over the network average degree $\langle k \rangle$ for 29 real network topologies. The black dashed line represents the least square regression line of the data.

very low correlation ($\rho = 0.15$) between $\langle k \rangle$ and μ.
Instead, we find that μ is well explained by the parameter

$$\beta = 1 - \frac{\sum_i |k^i_{\text{in}} - k^i_{\text{out}}|}{2L} \in [0, 1] \tag{4-2}$$

which takes the value of 1 for perfectly balanced graphs, that is, graphs for which the indegree k_{in} of each node is the same as its outdegree k_{out}. As shown in Fig. 4-3, β is correlated ($\rho = 0.79$) with μ. This is consistent with the theoretical background for our method provided by Hosoe's theorem [16] as a cycle partition of a network is a balanced digraph. Hence, we can view the parameter β as a measure of how efficiently the network connections are allocated as if an edge entering a node does not have as a counterpart an edge departing from the node it enters, then it cannot be used to find a cycle partition of a graph. The empirical correlation found between β and μ is also coherent with the fact that regular networks with $\langle k \rangle \geq 1$ and connected undirected networks, both characterized by balanced graphs, can be made controllable by means of only one control signal [37].
For the reader's convenience, the results shown in figure 4-3 are summarized in Table 4-1, where a complete list of the real network topologies analyzed, together with their number of nodes N, their permeability μ and the parameter β is given.
The network permeability μ, defined in Eq. (3) of the main text, is a property of the network structure. Coherently, μ is computed without taking into account the role played by the sets

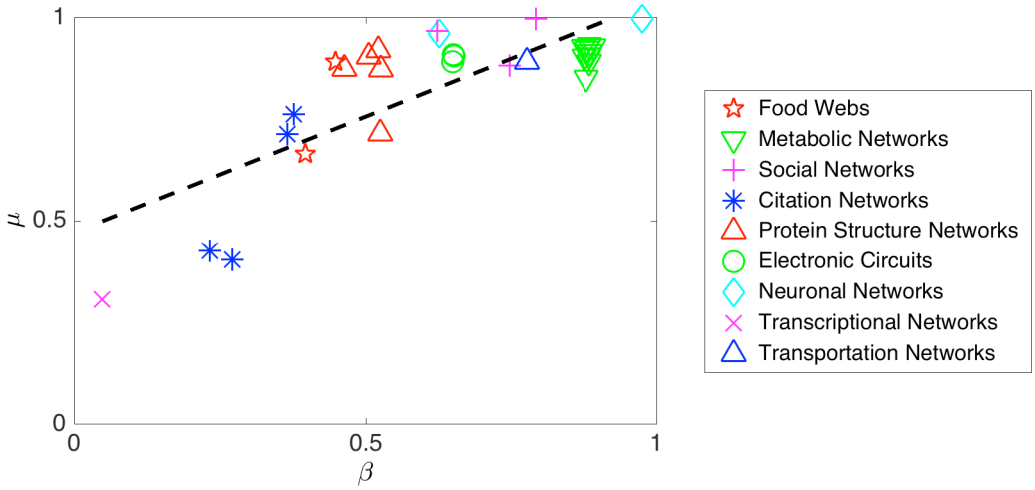

Figure 4-3: Plot of the network permeability μ over the parameter β for 30 real network topologies. The black dashed line represents the least square regression line of the data.

Ω, Φ, and Ψ, as reasonably the constraints on admissible, target and untouchable nodes are related to specific scenarios of application of our method. The permeability μ thus takes the limit value of 0 for an ensemble of disconnected nodes, as the diffusion of signals is prevented by the absence of connectivity and each node can be made controllable only if it is a driver. This corresponds to the worst case scenario in terms of permeability. Nevertheless, when the sets Ω and Ψ are considered, some nodes of the network become inaccessible directly and indirectly. Namely, in order to ensure the control signals do not reach the nodes of the set Ψ, all the untouchable nodes and all the nodes in their upstream cannot be selected as drivers. Hence, they can neither be made controllable directly nor indirectly. The same line of argument extends to the case of the admissible nodes. Namely, if a nodes is not part of the set Ω, nor it is accessible from a node of the latter set, then it can neither be made controllable directly nor indirectly. As for the presence of target nodes, while these do not affect our ability to control any specific node, their presence might make the optimization problem in (3-3)-(3-7) unfeasible. This corresponds to the situation in which there does not exists a set of driver nodes $\Omega_D \subset \Omega$ of dimension M that ensures structural controllability of the set of target nodes Φ.

Summing up, in the presence of untouchable and target nodes, and when the set of admissible nodes does not correspond to the entire set of network nodes, the (approximate) computation

Network	μ	N	β
Aeropyrum pernix Metabolic[24]	0.91	1057	0.88
Air Traffic Control [19]	0.89	1226	0.78
B cell Interactome [22]	0.87	5737	0.52
Budding Yeast [21]	0.16	2361	0.53
C. Elegans Metabolic [24]	0.91	1173	0.88
C. Elegans Neuronal I[20]	0.96	306	0.63
C. Elegans neurnoal II[25]	0.99	281	0.97
DBLP Citation [17]	0.42	12591	0.23
E. Coli Metabolic [24]	0.85	2275	0.88
Emericella Nidulans Metabolic [24]	0.92	916	0.88
Florida food web[21]	0.89	128	0.45
Little Rock Lake food web[17]	0.66	183	0.40
Mycobacterium Tubercolosis [24]	0.90	1520	0.87
Mycoplasma Pneumoniae Metabolic [24]	0.93	411	0.87
OC link social [20]	0.88	1899	0.75
Physicians Trust [18]	0.97	246	0.62
Protein Structure I[23]	0.92	95	0.52
Protein Structure II[23]	0.87	53	0.46
Protein Structure III[23]	0.90	99	0.50
Residence Hall Social [17]	0.99	217	0.79
s208 Electronic Circuit [23]	0.89	122	0.65
s420 Electronic Circuit [23]	0.91	252	0.65
s838 Electronic Circuit [23]	0.91	512	0.65
S. Cerevisiae Metabolic [24]	0.89	1511	0.88
Scientometrics Citation [21]	0.76	2729	0.38
Small World Citation [21]	0.40	395	0.27
Small World & Griffin citation [21]	0.71	1024	0.36
Thermotoga Maritima Metabolic [24]	0.93	830	0.89
Treponema Pallidum Metabolic [24]	0.93	485	0.88
TRN-yeast[23]	0.30	688	0.05

Table 4-1: List of real network topologies analysed.

of the integral in (4-1) can yield negative values. While this may seem incoherent, it well captures the fact that the constraints on the admissible, target and untouchable nodes can lead to a network being less propense to being controllable than an ensemble of disconnected nodes. To capture the impact of the sets Ω, Φ, and Ψ on the network permeability μ, we introduce the conditioned permeabilities $\mu(\Omega)$, $\mu(\Phi)$, and $\mu(\Psi)$ which are defined in the

interval $[-1, 1]$. We would like to stress that these indexes are properties of both the network and of the specific control problem that is addressed.

The conditioned permeability is computed by means of the same formula given in equation (4-1) where N is still the number of nodes of the network and M is the number of driver nodes deployed. The only difference is that $\mathcal{C}(M)$ is the result of an optimization problem where either the constraint on the untouchable, target, or admissible nodes is considered depending on whether we are computing $\mu(\Psi)$, $\mu(\Phi)$, or $\mu(\Omega)$, respectively. From a practical standpoint, as the presence of untouchable and inadmissible nodes constrains to select the set Ω_D out of a set Ω' that is only a subset of $\mathcal{V}$, the number of drive nodes M to be selected is bounded by $|\Omega'|$. Hence, in (approximately) computing the integral in equation (4-1), one must set $|\mathcal{C}(M)| = |\mathcal{C}(|\Omega'|)|$ for all values of M greater than $|\Omega'|$. Instead, in the presence of a set of target nodes Φ, if for a given M the optimization problem in (3-3)-(3-7) does not admit a solution, then in computing $\mu(\Phi)$ one must set $|\mathcal{C}(M)| = 0$.

To understand the impact of the presence of untouchable nodes on our ability to control a network, we evaluated the difference between the network permeability μ, and the conditioned permeability $\mu(\Psi)$. In a first round of numerical experiments, we have randomly selected, for each real network analyzed, 5% of its nodes to be untouchable and computed the conditioned permeability $\mu(\Psi)$. To ensure statistical significance of our numerical results, we have averaged the results over 50 different random selections of the set of untouchable nodes per network. Then, we have varied the dimension of the set of untouchable nodes to 10% of the network nodes again averaging the results over 50 different random selections of the set Ψ. We found that these impurities tend to jeopardize our ability to control a network, as a small set of untouchable nodes can be responsible for a large loss of permeability. This phenomenon in shown in panel **a** of Figure 4-4, where the relation between the parameter β and the average loss of permeability $\Delta\mu(\Psi)$ in the presence of a randomly chosen set of $0.05N$ nodes of each network is portrayed. In panel **b** of Figure 4-4 the same results are shown but relative to the scenario in which the dimension of the set Ψ is equal to $0.10N$. In both cases, we find a correlation between $\Delta\mu$ and β. Namely, when $|\Psi| = 0.05N$ we observe that $\rho = 0.81$ while when $|\Psi| = 0.10N$ we have that $\rho = 0.86$.

We also performed an additional set of analyses in which we reverted to a dimension of $0.05N$ untouchable nodes but considered four different selection criteria for the set Ψ. We randomly chose the untouchable nodes from

a) the nodes with low indegree (nodes with degree lower than the 33-rd percentile of the indegree distribution);

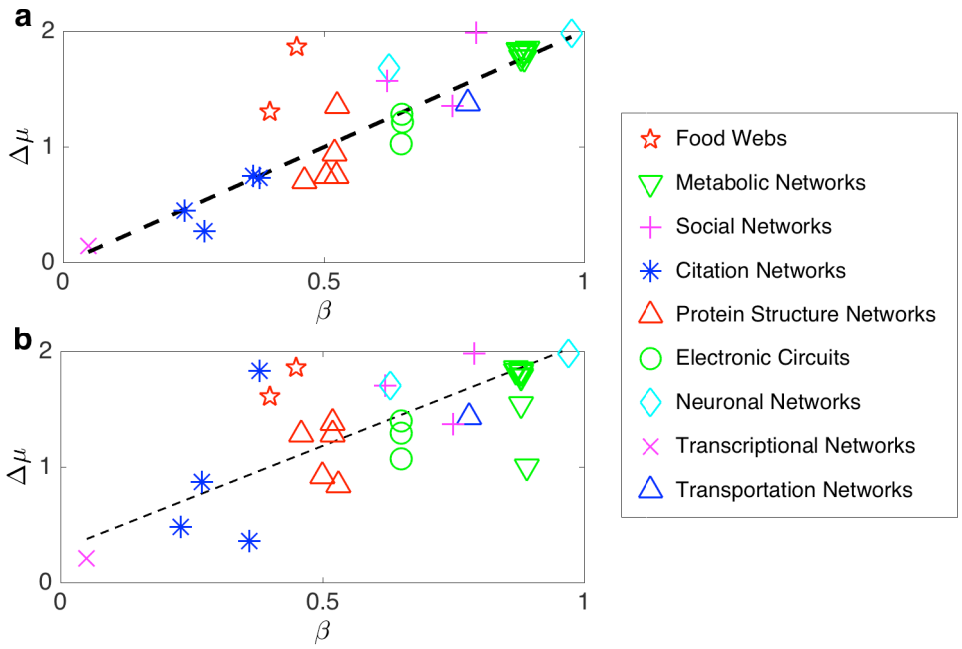

Figure 4-4: Plot of the loss of permeability $\Delta\mu(\Psi)$ over the parameter β when **a** we have that $|\Psi| = 0.05N$ and **b** we have that $|\Psi| = 0.10N$.

b) the nodes with low outdegree (nodes with degree lower than the 33-rd percentile of the outdegree distribution);

c) the nodes with high indegree (nodes with degree higher than the 67-th percentile of the indegree distribution);

d) the nodes with high outdegree (nodes with degree higher than the 67-th percentile of the outdegree distribution);

For each criterion and for each topology of a real network in our database, we performed 50 selections of the set Ψ and averaged the resulting conditioned permeabilities. We found that these differences are substantially smaller than the loss of permeability in the presence of a

completely random extraction of the set Ψ. Specifically, we found that

$$\left\langle \frac{(\Delta\mu(\Psi^a) - \Delta\mu(\Psi^r))^2}{(\Delta\mu(\Psi^r))^2} \right\rangle = 0.12,$$
$$\left\langle \frac{(\Delta\mu(\Psi^b) - \Delta\mu(\Psi^r))^2}{(\Delta\mu(\Psi^r))^2} \right\rangle = 0.02,$$
$$\left\langle \frac{(\Delta\mu(\Psi^c) - \Delta\mu(\Psi^r))^2}{(\Delta\mu(\Psi^r))^2} \right\rangle = 0.01,$$
$$\left\langle \frac{(\Delta\mu(\Psi^d) - \Delta\mu(\Psi^r))^2}{(\Delta\mu(\Psi^r))^2} \right\rangle = 0.04,$$

where:

- μ is the permeability of the network;
- $\Delta\mu(\Psi^i) = \mu - \mu(\Psi^i)$ is the permeability conditioned to the presence of untouchable nodes selected according to the i-th criterion;
- $\Delta\mu(\Psi^r) = \mu - \mu(\Psi^r)$ is the permeability conditioned to the presence of completely randomly selected untouchable nodes (the criterion used in the main text of the paper);
- $\langle\cdot\rangle$ indicates that the quantities are averaged over the networks in our databases and over 50 different extractions of the sets Ψ^i.

Moreover, Figure 4-5 shows that the correlation between the loss of permeability $\Delta\mu(\Psi^i)$ and β, when applied to all of the networks in our dataset, is confirmed, irrespective of the specific selection criterion considered. In fact, $\Delta\mu(\Psi^a)$, $\Delta\mu(\Psi^b)$, $\Delta\mu(\Psi^c)$, and $\Delta\mu(\Psi^d)$ have a correlation with β of 0.86, 0.86, 0.84, and 0.85, respectively.
The previous numerical analyses were aimed at uncovering the relation between the network structure and its readiness to be made controllable regardless of the number of drivers deployed for the task. The shift of perspective proposed in this thesis, from complete to partial controllability, and the associated toolbox of algorithms presented in chapter 3 allow us to also uncover the structural features of the network nodes that determine their controllability properties. By solving the optimization problem in equations (3-3)-(3-7) without restrictions on the set of admissible, target, and untouchable nodes we can obtain the full composition of the set of controllable nodes $\mathcal{C}(M)$ and of its complement $\bar{\mathcal{C}}(M)$. In performing our numerical studies, we kept track of the structural properties of the nodes of these sets in order to uncover the structural properties of the nodes that can be made easily controllable. We found that the nodes of both $\mathcal{C}(M)$ and $\bar{\mathcal{C}}(M)$ are characterized by signatures. Namely, the

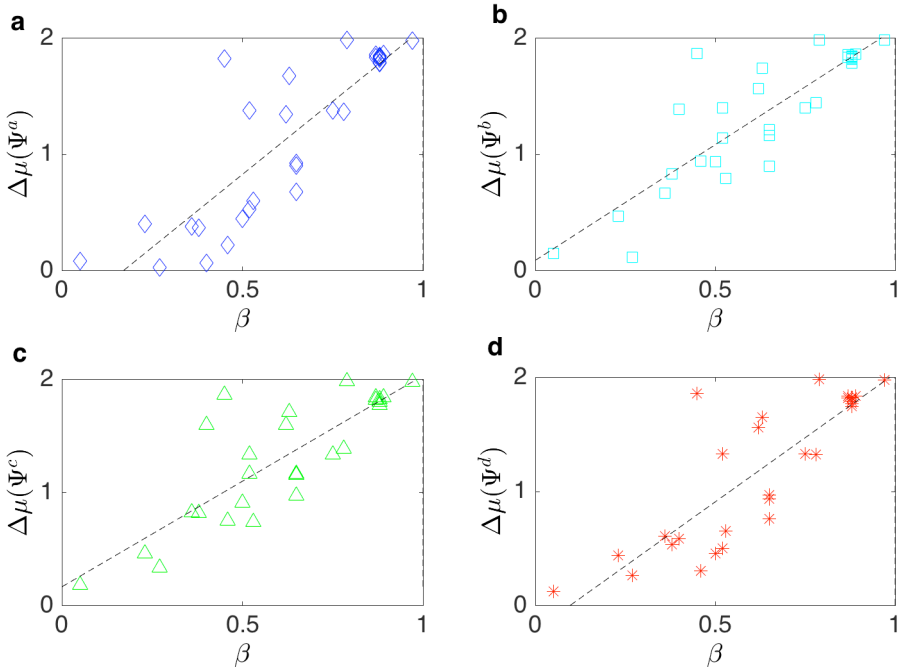

Figure 4-5: Plot of the loss of permeability $\Delta\mu(\Psi)$ over the parameter β. The title of each panel corresponds to the criterion with which the set of untouchable nodes responsible of the loss of permeability was selected.

nodes of $\mathcal{C}(M)$ exhibit higher degree than those of its complement $\bar{\mathcal{C}}(M)$ as shown in Fig. 4-6(a).

After having structurally characterized the nodes that tend to fall in the set $\mathcal{C}$ from those that require a large number of driver nodes to be included in the optimal set of controllable nodes, we turn our attention to the structural properties of the set of optimal driver nodes Ω_D. In ref [37], Liu et al. found that when applying the maximal matching algorithm, input signals were usually injected in nodes with low degree. This finding is labeled as *surprising* as the authors expected the hubs to play a key role in network control. Being able to select optimal sets of driver nodes Ω_D of any dimension in the interval $[0, N]$, allows us take a step forward in the analysis of the structural properties of the optimal driver nodes. By observing Figure 4-1, we note that for small values of M the marginal increments in the dimension of the set of controllable nodes $|\mathcal{C}(M)| - |\mathcal{C}(M-1)|$ are larger than those that are experienced when M is large. This spurs us to study the structural properties of the nodes that are selected as drivers when M is small, as these often allow controlling a large fraction of the network nodes. We find that when M is small, the nodes of $\Omega_D(M)$ typically

exhibit low indegree and high outdegree as shown in Figure 4-6(a) for the Small World and Griffith citation network. When nodes with this signature lack, then nodes with both low indegree and low outdegree are selected first. This observation is coherent with Lemma 3.2.1

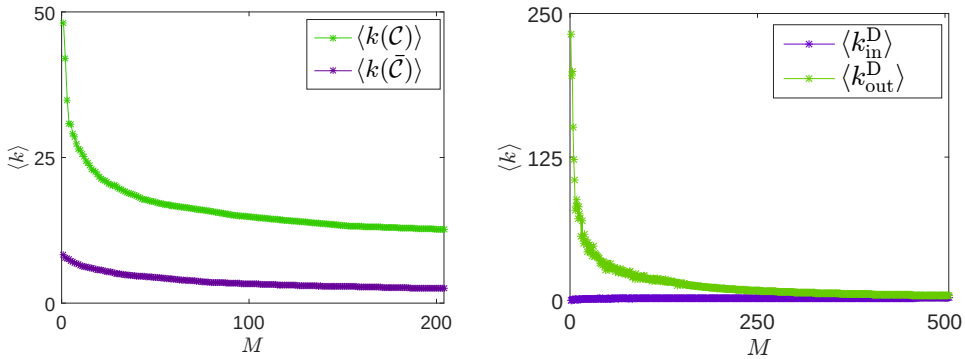

(a) (b)

Figure 4-6: (a) Plot of the outdegree (green) and indegree(magenta) of the optimal driver nodes. (b) Plot of the average degree of the nodes of $\mathcal{C}$ (green) and of the nodes of $\bar{\mathcal{C}}$ (magenta) over M. Then former exhibit higher degree than the latter.

which provides the theoretical foundation of the toolbox of driver node selection algorithms presented in Chapter 3. Specifically, to generate a large set of controllable nodes, a driver must have many large cycles in its downstream and a long stem must depart from it. Clearly, if a node v_i has non-zero indegree then there exists at least a node v_j (among those in the upstream of v_i) such that the longest stem originating from v_j is longer than (or equal to) the longest stem originating in v_i. Moreover, if a network graph has roots with many nodes in their downstream, then these roots are likely to also have many cycles in their dowsntream. Among the nodes with low indegree, those with high outdegree guarantee more degrees of freedom in determining the longest stem originating from them and are more likely to have many nodes, and thus also many large cycles, in their downstream. Hence, the empirical observation that the optimal driver nodes have low indegree and high outdegree is coherent with Lemma 3.2.1. From these considerations, the question arises of how these new results match with those in ref [37]. Luckily, the answer is somewhat straightforward and can be deducted from Figure 4-1, where we observe that when M is large the marginal increment $|\mathcal{C}(M)| - |\mathcal{C}(M-1)|$ becomes smaller and smaller. This means that when M is large every additional driver only allows controlling a small number of new nodes. In analyzing most

networks, we have experienced the somewhat paradoxical condition that when M is increased $|\mathcal{C}(M)| - |\mathcal{C}(M-1)| = 1$. The network motif that generates this condition is the so called dead end, that is, an external dilation where at least one of the two stems of the branching is made of only one node. When this motif occurs, which is very common especially in scale-free networks as these have several nodes with low degree [3], the one node stem must be directly controlled. When aiming at ensuring complete controllability of a network, an extensive deployment of the driver nodes is required to directly control the dead ends of the network topology. As these dead ends have zero indegree, this substancially lowers the average outdegree of the set of nodes where input signals must be placed.

Our findings on the signatures of the nodes of the sets Ω_D and $\mathcal{C}$ have immediate practical relevance. First, the signature of the nodes of $\mathcal{C}(M)$ points out that targeting nodes with low degree requires a large number of drivers, while targeting nodes with high degree is feasible with a small set Ω_{D}. On the other hand, the signature of the nodes of $\Omega_{\mathrm{D}}(M)$ indicates that when lacking the ability to conduct the permeability analysis described above, a good criterion for the selection of the driver nodes is to choose, amongst the nodes with low indegree, those with high outdegree.

Altogether, the results of our permeability analysis of several real network topologies provide tools for an easy assessment of how challenging it is to fulfill given controllability requirements. If a network is characterized by a low value of β, the set of admissible nodes does not encompass nodes with low indegree and high outdegree, and the nodes to be targeted have small degree k, then even fulfilling the mildest controllability requirements might be a chimera. Conversely, high controllability goals can be achieved when these conditions are not verified.

Our results show that a large set of controllable nodes can be obtained with a reasonable amount of drivers only when the network structure determines a high permeability. When does this reasonable amount reduce to a handful of nodes thus knocking down the control costs? We find the answer to this question by classifying networks on the basis of two measures, their permeability μ and the maximum centrality $\mathcal{C}(1)$ of their nodes. It follows that networks can be divided into three classes (see Fig. 4-7) the first encompassing highly permeable networks ($\mu > 0.5$) having at least a node with high centrality ($|\mathcal{C}(1)| > 0.5$), the second encompassing highly permeable networks that do not have a node with high centrality, and the third class encompassing impermeable networks that do not have a node with high centrality. The networks in the first class are such that a large set of controllable nodes $\mathcal{C}$ can be obtained inexpensively, that is, by using only a handful of drivers. For networks belonging to the second class, a large $\mathcal{C}$ can still be obtained, but at a higher price,

as $\mathcal{C}(1)$ is small but increases rapidly with the number of drivers. Finally, networks in the third class tend to be impermeable to control signals regardless of M. For these networks, only mild contollability requirements can be fulfilled and at a high price and the role played by the sets of target, admissible and untouchable nodes is critical. Figure 4-7 also shows that the topology of networks that share the same functions (in particular, protein networks, metabolic networks, and electric circuits) tend to fall in the same class.

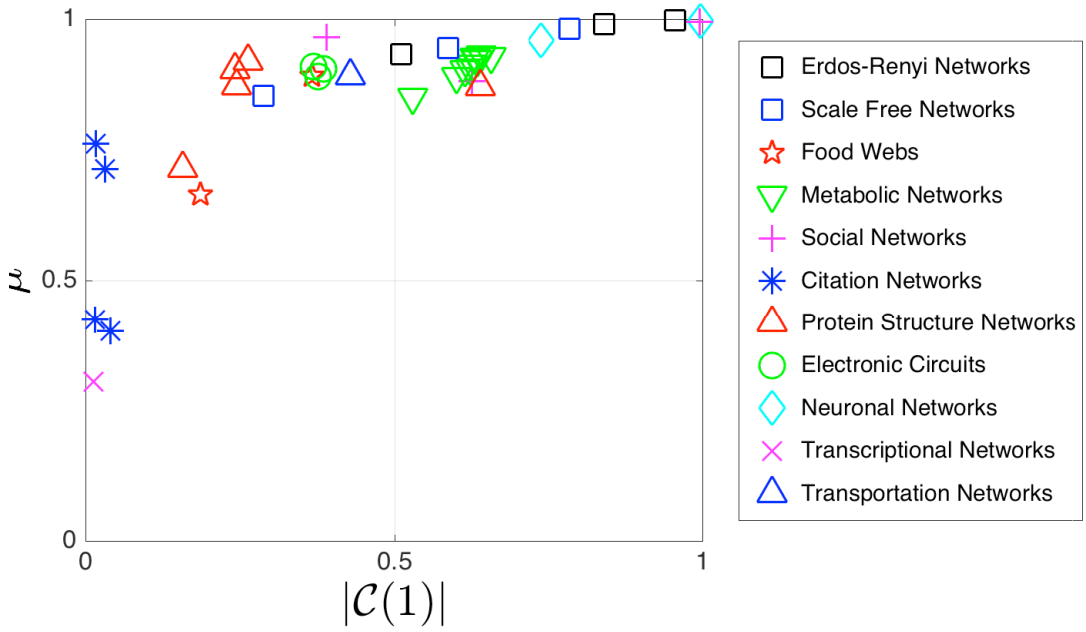

Figure 4-7: Plot of the relation between the network permeability μ and the maximum centrality $|\mathcal{C}(1)|$ of its nodes.

In this chapter, we have leveraged the toolbox of algorithms presented in chapter 3 to analyze several real and model network topologies in order to uncover the relation between the network degree distribution and its permeability. Moreover, we have studied the structural properties of the nodes of the sets $\mathcal{C}$ and Ω_D finding that these are characterized by signatures. In the next chapter, we will show how these results can be exploited to design heuristic driver node selection strategies for huge complex networks. Before doing so, we would like to emphasize a few methodological aspects of the numerical analysis performed in this chapter.

Generation of model topologies Scale Free topologies were generated by means of the directed version of the so called static model [14]. All numerical results on artificial networks

are averaged over 100 topologies of 1000 nodes each.

Integer Linear Programming solver The numerical analysis was conducted on the Matlab platform by using the integer linear programming solver intlinprog or the Gurobi add-on. We emphasize that the method we propose can be implemented also on other available commercial software. All the presented results are exact as we have never been forced to settle for an approximation of the optimal solution due to limitations on the execution time of our algorithm.

CHAPTER 5

Heuristic Driver Node Selection Strategies

In Chapter 4 we have performed an analysis of several real and model networks in order to uncover the structural properties that influence the network permeability μ. In doing so, we also kept track of the characteristics of the nodes of the optimal set of drivers Ω_D and of the resulting set of controllable nodes $\mathcal{C}(M)$. In this chapter, we take advantage of the findings described in Chapter 4 to design heuristic driver node selection strategies that exploit the network structure in order to maximize the number of controllable nodes. We will thus refer to the optimization problem in equations (3-3)-(3-7) without taking into account the constraints on admissible, target, and untouchable nodes.

The main goal of the proposed heuristic strategies is twofold. First of all, although we never ran into an unsolvable instance of the ILP in equations (3-8)-(3-12), that is, the dreaded worst-case scenario which could arise due to its NP-hard nature, we aim at providing the readership with a sub-optimal strategy should this case arise. Secondly, as is the case for all graph-optimization problems, the scale of our ILP grows with the dimension of the network. As we will see, the strategies proposed in this chapter allow reducing the scale of the optimization problem to be solved.

We start discussing our heuristic strategies by recalling that the ILP in equations (3-8)-(3-12) is made NP-hard by the constraints in equation (3-12). These constraints only ensure that all the elements of the set of controllable nodes be accessible from the driver nodes. On the other hand, finding an optimal cycle partition of a graph, that is, the task performed in equations (3-8)-(3-11), can be performed in polynomial time. Hence, in our heuristic strategies we aim at decoupling these two tasks. To do so, we start by recalling that according to Lemma 3.2.1, for a node to be controllable, it must either be part of a stem originating from a driver

node or part of a cycle accessible from a driver node. As all of the nodes of a stem are accessible from its source by definition, the accessibility constraints in equation (3-12) only come into play if the graph of a network contains cycles. Otherwise they are redundant and do not alter the polytope defined by the constraints in (3-10),(3-11). As we have shown that the matrix defined by the latter constraints is totally unimodular we can give the following Lemma.

Lemma 5.0.1. *If the graph $\mathcal{G}$ of a network is a DAG, then the ILP in equations* (3-8)-(3-12) *that must be solved in order to select a set of driver nodes of fixed cardinality M to maximize the number of controllable nodes is not NP-hard.*

The relevance of Lemma 5.0.1 goes beyond its statement in it allows tailoring an heuristic strategy to networks that encompass very few, small cycles.

Heuristic Strategy 1: If the maximum number of nodes of a network that can be included in disjoint cycles by only leveraging the network graph $\mathcal{G}$ is small, then a good heuristic strategy for selecting the driver nodes so to maximize the number of controllable nodes can be obtained by applying the algorithm for the exact solution of our problem while neglecting the constraints in equation (3-12) *and then removing, from the resulting stem-cycle disjoint subgraph, the cycles that are not accessible from the drivers. We will denote the set of controllable nodes obtained leveraging on Heuristic Strategy 1 by $\mathcal{C}^1(M)$*

The rationale behind this heuristic strategy is very simple. If the network graph is such that very few of its nodes can be included in disjoint cycles, than we may as well relax the accessibility constraints and solve a problem that is not NP-hard. This will lead to a slight overestimation of $|\mathcal{C}|$ as some inaccessible cycles might be included in the stem-cycle disjoint subgraph resulting from the solution of the relaxed ILP. Nevertheless, by eliminating the inaccessible cycles we should obtain a set of controllable nodes $\mathcal{C}^1(M)$ the dimension of which should be close to the actual optimal solution $\mathcal{C}^*(M)$.

As we have anticipated, Heuristic Strategy 1 is to be used if only a small number of nodes can be included in disjoint cycles by only leveraging the edges of the graph of the network. While we will leave to later the explanation of the criteria based on which one can determine whether the number of nodes that can be included in disjoint cycles is neglectable, a key aspect that must be immediately discussed is how to determine this number. One trivial way, is to apply Algorithm 1 assuming $M = 0$ and neglecting the accessibility constraints in equation (3-12) when solving the ILP (which thus becomes of complexity P). While this strategy allows exactly computing the number of nodes that can be included in disjoint

cycles, it requires solving an LP with $|\mathcal{P}| + |\mathcal{V}|$ decision variables (all the network edges plus an additional number of self loops equal to the number of nodes of the network) and $2|\mathcal{V}|$ constraints, two for each network node. Taking into account that it is unknown whether LPs can be solved in strongly polynomial time, this might be inefficient. An upper bound for the number of nodes that can be included in disjoint cycles can be obtained instead by finding all the network's Strongly Connected Components (SCCs) and taking, as the bound, the number of nodes contained in SCCs encompassing more than one node. The advantage is that finding the SCCs of a graph is a task that can be performed with Tarjan's algorithm which requires a running time of $O(|\mathcal{V}| + |\mathcal{P}|)$ [63], that is, linear in the number of nodes and edges of the network graph.
The performance of Heuristic Strategy 1 essentially depends on

a) whether the actual optimal solution encompasses most of the very few network nodes that can be included in disjoint cycles by only leveraging the edges of the network graph;

b) whether these nodes are accessible from the driver nodes selected by Heuristic Strategy 1.

While none of these two factors are under our control, we can derive two bounds on their effect. The derivation of both bounds is simple and relies on the fact that the optimal value of any relaxation of an optimization problem is an upper bound for the optimization problem itself. Hence, to find the first bound we shall simply apply Hueristic Strategy 1 and take the difference between the dimension of the stem-cycle disjoint subgraph before and after the elimination of the inaccessible nodes as a bound for the difference between the optimal value $|\mathcal{C}^*(M)|$ and $|\mathcal{C}^1(M)|$.
Obtaining the second bound is equally simple in it implies solving a different relaxation of our ILP, this time ignoring the integer constraint on the decision variables. The bound on the error is then obtained as the difference between the optimal value of this relaxation and $|\mathcal{C}^1(M)|$.
Heuristic Strategy 1 is based on adapting the optimal strategy that should be used when the network graph is a DAG to the case in which the number of cycles is neglectable with respect to the number of the network nodes. Before going through the next heuristic strategy, let us treat the opposite scenario, that is, the case in which the network graph is made of only one Strongly Connected Component. While this case is exactly the opposite of that in which the network graph is a DAG, it can be treated exactly in the same way. Namely, as in an SCC, by definition, any node is accessible from any other one, the constraints in equation

(3-12) are redundant. Thus again thanks to the total unimodularity of the matrix defined by equations (3-10) and (3-11) we can give the following Lemma.

Lemma 5.0.2. *If the graph $\mathcal{G}$ is made of only one SCC, then the ILP in equations* (3-8)-(3-12) *that must be solved in order to select a set of driver nodes of fixed cardinality M to maximize the number of controllable nodes is not NP-hard.*

Lemma 5.0.2 also applies to the case in which the network graph is made of a giant strongly connected component plus an arbitrary number of one-node SCCs without self loops in the upstream of the giant component. In this case, as the giant component is the only SCC encompassing disjoint cycles, and as all of its nodes are accessible from all the network nodes, the accessibility constraints in equation (3-12) are still redundant.
After having treated the two opposite scenarios of network graphs that are either DAGs or made of one SCC together with two scenarios in which the network topology is close to fulfilling one of these two conditions, let us turn our attention to the general case in which the network graph is made of several SCCs each of at least two nodes and thus encompassing cycles. As anticipated, in this case the idea is to decouple the accessibility problem from that of finding an optimal cycle partition of a graph, that is, the two tasks performed by the ILP in equations (3-8)-(3-12).

Heuristic Strategy 2: If the network graph is made of several SCCs each with more than two nodes, then a good heuristic strategy is to place at least a fraction of the M driver nodes in the Root Strongly Connected Components that have the largest number of nodes in disjoint cycles in their downstream.

Deploying Heuristic Strategy 2 is not as straightforward as deploying Heuristic Strategy 1, and thus we will now go through the details of its steps. The general idea is that when M is small and the network is cycle rich then the relevance of the cycles in the largest stem-cycle disjoint subgraph originating from the driver nodes (Γ_c) is much larger than that of the M stems. Hence, placing the driver nodes in the RSCCs that have a large number of cycles in their downstream ensures the heuristic strategy defines a large stem-cycle disjoint subgraph $\bar{\Gamma}_c$ as its dimension will be at least equals to the number of nodes in these cycles. Before giving the algorithm required to deploy Heuristic Strategy 2 we must define the following notation:

- we denote by $\mathcal{S} = \{s_i\}$ the set of SCCs of a graph.
- we denote by $\mathcal{R} = \{r_i\} \subset \mathcal{S}$ the set of RSCCs of a graph.

- we denote by $|s_i|$ the maximum number of nodes of the SCC s_i that can be included into disjoint cycles;
- we denote by $\Delta(r_i)$ the set of SCCs in the downstream of the RSCC r_i, including r_i.
- we denote by $|\Delta(r_i)|$ the maximum number of nodes of the SCCs in $\Delta(r_i)$ that can be included in disjoint cycles.

Algorithm 2

1. Find the set $\mathcal{S}$ of the SCCs of the network graph.
2. $\forall\ s_i \in \mathcal{S}$, find the maximum number of nodes of s_i that can be included in disjoint cycles ($|s_i|$). We remark that this can be done by deploying Algorithm 1 skipping steps $2-7$ and ignoring the constraint in equation (3-12) in the ILP (which can thus be relaxed to a Linear Program).
3. $\forall\ r_i \in \mathcal{R}$, find the maximum number of nodes in its downstream that can be included in disjoint cycles ($|\Delta(r_i)|$). We underline that $|\Delta(r_i)| = \sum_{j:s_j \in \Delta(r_i)} |s_j|$, that is $|\Delta(r_i)|$ is equal to the sum of the $|s_j|$ for all the SCCs s_j that are in the downstream of the RSCC r_i.
4. Define the set $D = \emptyset$.
5. Define the set $R = \mathcal{R} - \cup_{i:|\Delta(r_i)=0|}(r_i)$. The set R includes all the elements of $\mathcal{R}$ with at least a cycle in their downstream.
6. Select, out of the set R, the RSCC $r^* = \arg\ \max_{r_i \in R}(|\Delta(r_i)|)$.
7. Add r^* to the set D.
8. Remove r^* from the set R, that is, $R = R - r^*$.
9. Remove, from all the sets $\Delta(r_i) : r_i \in R$, all the SCCs s_i that are in the downstream of r^*.
10. Recompute $|\Delta(r_i)|$ for all $r_i \in R$ as

$$|\Delta(r_i)| = \sum_{j:s_j \in \Delta(r_i)} |s_j|. \tag{5-1}$$

11. remove, from the set R all the elements r_i such that $|\Delta(r_i)| = 0$

12. repeat steps 6 to 10 until the number of elements in D is equal to M, that is, the constraint on the number of driver nodes or until the set R is empty.

13. $\mathcal{G}' = \mathcal{G}$.

14. Remove from $\mathcal{G}'$ all the nodes that are not either i. nodes of the RSCCs in the set D or ii. in the downstream of the RSCCs in the set D.

15. Define the scalar $N = |\mathcal{V}'|$. N is equal to the number of nodes of the graph $\mathcal{G}'$.

16. Find the set $\Omega' = \{\cup_{i|v_i \in v_i \in r_j \in D}\}$.

17. Add, to $\mathcal{G}'$ a new node, say $N + 1$.

18. Add $|\Omega'|$ new edges exiting node $N + 1$ and entering each node of Ω'.

19. Add N new edges exiting each node of $\mathcal{G}'$ and entering node $N + 1$.

20. Add N self loops, one for each node of $\mathcal{G}'$ except for node $N + 1$.

21. Associate a binary decision variable y_{ij} to each edge p'_{ij} of $\mathcal{G}'$.

22. Associate a unit weight w_{ij} to each decision variable y_{ij} that is either:
    - associated with an edge p'_{ij} of $\mathcal{G}'$ that is also an edge of $\mathcal{G}$;
    - associated with an edge p'_{ij} of $\mathcal{G}'$ that exits node $N + 1$;

23. Associate zero weight w'_{ij} to all the other decision variables y_{ij}:

24. Solve the following Linear Program:

$$\max_{y} \quad \sum_{i} \sum_{j} w'_{ij} y_{ij} \tag{5-2}$$

subject to

$$y_{ij} \in [0, 1] \quad \forall i, j | p'_{ij} \in \mathcal{P}' \tag{5-3}$$

$$\sum_{j} y_{ij} = 1 \quad \forall i = 1, ..., N \tag{5-4}$$

$$\sum_{i} y_{ij} = 1 \quad \forall j = 1, ..., N \tag{5-5}$$

$$\sum_{i: v_i \in d_j} y_{i,N+1} = 1 \; \forall j = 1, ..., M \tag{5-6}$$

While Algorithm 2 is very lengthy, Heuristic Strategy 2 is actually very simple. As anticipated, the rationale is that selecting as a driver a node in an SCC s_i or in its upstream allows controlling at least a number of nodes equal to $|s_i|$ as all the cycles of s_i will be accessible from the selected driver node. Hence, one would ideally want to select as drivers the nodes that are encompassed in cycle rich SCCs but most importantly in SCCs that have cycle rich downstreams. So the question shifts to which SCCs have the richest downstream in terms of nodes that can be included in disjoint cycles. To answer this question, we can rely on the DAG condensation of the network graph. In this new acyclic graph, there is an edge connecting SCC s_i to SCC s_j if, in the graph of the network $\mathcal{G}$, there exists a directed path from the nodes of s_i to the nodes of s_j. The source nodes of the condensed graph correspond to the RSCCs of the graph $\mathcal{G}$. An example of a model network and of its DAG condensation is provided in Figures 5-1(a) and (b).

As any non root SCC is in the downstream of at least an RSCC, then the SCCs with the richest downstream in terms of nodes that can be included in disjoint cycles are indeed the RSCCs, or, equivalently, the source nodes of the DAG condensation of $\mathcal{G}$. Hence, Heuristic Strategy 2 will select as drivers only the nodes of the RSCCs of the graph $\mathcal{G}$. Among these RSCCs, those with the richest downstream will be privileged. To do so, (steps 1 and 2) we first find the set $\mathcal{S}$ of all the SCCs of the network and for each s_i we compute the value $|s_i|$, that is the maximum number of nodes of the SCC s_i that can be included in disjoint cycles. Then, in step 3, we isolate the set of RSCCs $\mathcal{R}$ and for each of its elements r_i we compute the maximum number of nodes of their downstream that can be included in disjoint cycles $|\Delta(r_i)|$. This can be done by simply adding up all the $|s_j|$ of the SCCs in the downstream of each root r_i. After having defined the sets D and R (steps 4 and 5), in step 6 we take the RSCC r^* that has the largest $|\Delta(r_i)|$ and add it to the set of RSCCs D out of which the drivers will be selected. As one driver node per RSCC r_i is sufficient to ensure controllability of the nodes of the SCCs in the set $\Delta(r_i)$, we must select M RSCCs to compose the set D as only one driver node will be selected out of each element of D. To do so, once the first element of D has been selected (step 7), in steps 8 we remove it from the set R. Then, in step 9 we remove all of its downstream from all the sets $\Delta(r_i)$ $r_i \neq r^*$ and in step 10 we update the values of $|\Delta(r_i)|$ $r_i \neq r^*$. Finally, we select, out of the remainder of the RSCCs, the one with the largest associated $|\Delta(r_i)|$. This procedure is repeated until the set D is composed of M elements or until the set R of the RSCCs which have at least a cycle in their downstream is empty.

From a conceptual standpoint, this iterative procedure can be viewed as a problem on a new graph composed of two levels: one including the RSCCs such that $|\Delta(r_j) \neq 0|$ and another

including the non root SCCs such that $|s_i| \neq 0$. In this new graph, we can only have edges connecting RSCCs to non root SCCs. Namely, an edge will connect RSCC r_i to SCC s_j if s_j is in the downstream of r_i. The problem on this new graph consists in selecting the RSCC that has in its downstream the SCCs with the largest number of nodes that can be included in disjoint cycles, updating the graph by eliminating the selected root, its downstream, and if necessary all the roots that no longer have $SCCs$ in their dowstream, and finally repeating these two steps until either M RSCCs have been selected or the new graph is empty. The reduced graph for the model network in Figure 5-1(a) is shown in Figure 5-1(c). The red circles correspond to the RSCCs while the blue circles to the non root SCCs.

Having defined the set D of the RSCCs in which the driver nodes will fall implicitly defines the set of nodes that will be accessible from the driver nodes. Namely, these can be obtained by taking the nodes of the RSCCs in the set D together with all the nodes in their downstream. The a priori knowledge of the nodes that will be accessible from the drivers allows us to ignore the accessibility constraints of the ILP in Algorithm 1. These must be substituted by an additional set of constraints, those in equation (5-6), that ensure a driver node is selected in each of the RSCCs of the set D. This time, the set of constraints in equations (5-4)-(5-6) defines a totally unimodular matrix as it fulfills the conditions given in ref [30]. Moreover, as the constant terms are integers, the ILP in equations (5-7)-(5-6) is not NP-hard.

Once we have selected the RSCCs in which the drivers will fall, we must proceed to the selection of these drivers and of the set of controllable nodes $\mathcal{C}$. This is done in steps 13 to 24 by simply specifying Algorithm 1 to the case in which a driver node must fall in each RSCC of the set M. Note that the a priori knowledge on the set of nodes that will be accessible from the drivers not only ensures the ILP is not NP-hard but reduces the number of decision variables and constraints of the optimization problem. This as all the nodes of the graph $\mathcal{G}$ that are not accessible from the drivers will certainly not be controllable and thus can be eliminated from the graph $\mathcal{G}'$ together with all their associated edges. Figure 5-1(d) shows the graph of the same model network in Figure 5-1(a). This time, the nodes selected as drivers are highlighted in green while the nodes accessible from the drivers are highlighted in yellow. The blue circles represent the nodes that are inaccessible from the drivers and thus will not be included in the graph $\mathcal{G}'$.

For the sake of simplicity and clarity Steps 13 to 24 refer to the case in which the number of elements of D is equal to M and not all the nodes of the network that can be included in disjoint cycles are in the downstream of the RSCCs where the driver nodes will fall. If instead all the nodes of the network that can be included in disjoint cycles are in the downstream of the RSCCs of the set D, we can revert to considering, in the graph $\mathcal{G}'$, the entire network

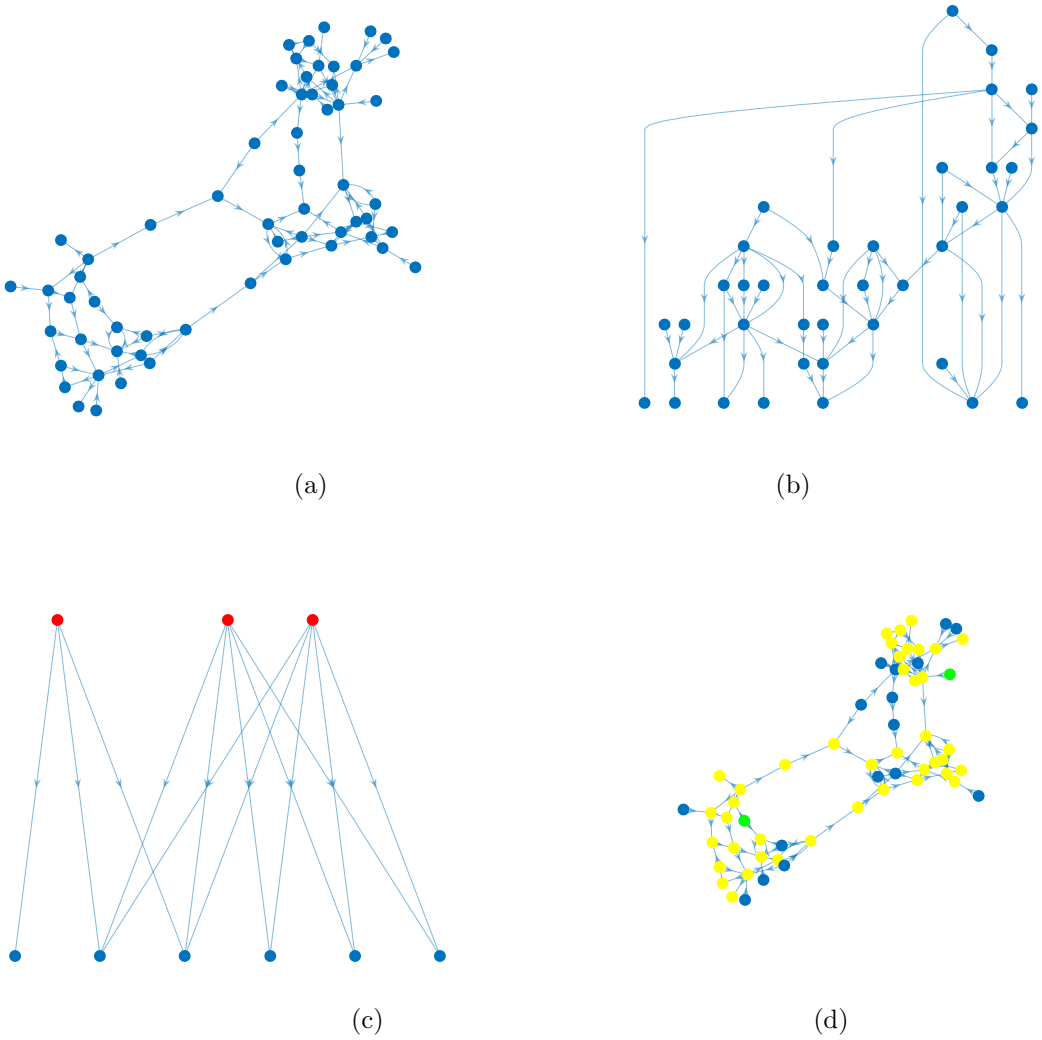

(a) (b)

(c) (d)

Figure 5-1: (a) The graph of a model network. (b) the DAG condensation of the model network. (b) The two-level reduced graph. Red circles represent RSCCs r_i such that $|\Delta(r_i)| \neq 0$, the blue circles represent SCCs s_i such that $|s_i| > 0$. (d) Green circles represent the nodes selected as drivers while yellow circles represent the nodes accessible from the drivers. The blue circles represent the nodes that are inaccessible from the drivers.

topology without taking into account the accessibility constraints. This as by ensuring at least a driver is selected in each RSCC of the set D guarantees all the disjoint cycles are accessible from the drivers. Note that less than M driver nodes might be required in order to ensure all the nodes in disjoint cycles be in the downstream of drivers. In this case, we

will have that $|D| < M$ and thus $M - |D|$ driver nodes can be freely selected. To do so, we take the set of $|D|$ drivers, say $\bar{\Omega}_D$, obtained after step 24 of Algorithm 2 and perform the following steps in order to add $|D| - M$ new drivers to the set $\bar{\Omega}_D$.

25 $\mathcal{G}' = \mathcal{G}$.

26 Add, to $\mathcal{G}'$ a new node, say $N + 1$.

27 Add N new edges exiting node $N + 1$ and entering each node of $\mathcal{G}'$.

28 Add N new edges exiting each node of $\mathcal{G}'$ and entering node $N + 1$.

29 Add N self loops, one for each node of $\mathcal{G}'$ except for node $N + 1$.

30 Associate a binary decision variable y_{ij} to each edge p'_{ij} of $\mathcal{G}'$.

31 Associate a unit weight w_{ij} to each decision variable y_{ij} that is either:

- associated with an edge p'_{ij} of $\mathcal{G}'$ that is also an edge of $\mathcal{G}$;
- associated with an edge p'_{ij} of $\mathcal{G}'$ that exits node $N + 1$;

32 Associate zero weight w'_{ij} to all the other decision variables y_{ij}:

33 Solve the following Linear Program:

$$\max_{y} \quad \sum_{i} \sum_{j} w'_{ij} y_{ij} \tag{5-7}$$

subject to

$$y_{ij} \in [0, 1] \quad \forall i, j | p'_{ij} \in \mathcal{P}' \tag{5-8}$$

$$\sum_{j} y_{ij} = 1 \quad \forall i = 1, ..., N \tag{5-9}$$

$$\sum_{i} y_{ij} = 1 \quad \forall j = 1, ..., N \tag{5-10}$$

$$\sum_{j} y_{N+1,j} = M \tag{5-11}$$

$$\sum_{i: v_i \in \bar{\Omega}_D} y_{i,N+1} = |D| \tag{5-12}$$

$$\sum_{i: v_i \notin \Omega_D} y_{i,N+1} = M - |D| \tag{5-13}$$

Equations (5-12) and (5-13) of the ILP defined in step 33 ensure each node of $\bar{\Omega}_D$ is a driver nodes that the other $M - |D|$ drivers are freely selected out of the remainder of the network nodes.

5.1 Performance Evaluation of Heuristic Strategy 2

In the first part of this chapter, we have defined two heuristic strategies belonging to the complexity class P able of coping with the problem of selecting M driver nodes in order to maximize the number of controllable nodes of a network $|\mathcal{C}|$. We showed that a priori, a lower bound for the performance of Heuristic strategy 1 can be computed given the number of network nodes that can be included in disjoint cycles as this heuristic strategy simply consist in finding the largest stem-cycle disjoint subgraph of the network graph and then eliminating the cycles that are not accessible from the drivers. Hence, as we are given the freedom of choosing which heuristic to use based on the network topology we are coping with, we have all the elements to decide whether Heuristic Strategy 1 fits our needs. Namely, given a network topology, the larger the number of nodes that can be included in disjoint cycles, the larger the error we are implicitly accepting in deploying Heuristic Strategy 1.
Differently from the case of Heursitc Strategy 1, evaluating the performance of Heuristic Strategy 2 is nontrivial. A posteriori, we can always evaluate the difference between the heuristic solution and the solution obtained by deploying Algorithm 1 while solving the LP relaxation of the optimization problem in equations (3-8)-(3-12). While on one hand this procedure gives us an uncertainty interval on the optimal value $|\mathcal{C}^*(M)|$, on the other hand little can be said without deploying both the heuristic strategy and Algorithm 1 relaxing the integer constraints of the ILP. Unfortunately, this can be a very lengthy procedure. It is thus interesting to perform a numerical analysis in order to compare the results of Heuristic Strategy 2 to that of Algorithm 1. In this numerical analysis we aimed at considering networks with different topological features so to provide a clear picture of the performance of our the proposed heuristic. We start our numerical analysis by considering the topology of the Cora citation Network [60, 17]. The topological features of this network are resumed in Table 5-1.

$\lvert\mathcal{V}\rvert$	23166
$\lvert\mathcal{P}\rvert$	91500
$\lvert\mathcal{S}\rvert$	18061
$\lvert\mathcal{R}\rvert$	9396

Table 5-1: Main topological features of the Cora citation Network

This network is characterized by a reasonably large number of SCCs compared to the number of network nodes. Nevertheless, of these 18061 SCCs one is a giant component made of 3991 nodes, the second largest being made of only 19 nodes. For this network, the maximum

number of nodes that can be included in disjoint cycles is 3973, 2342 of which lie in the giant component. For the Cora citation network, we have elected to solve the problem of selecting M driver nodes so to maximize $|\mathcal{C}|$ for M in the interval of integers [1 150] leveraging both Algorithm 1 and Heuristic Strategy 2. As shown in Figure 5-2, when coping with this network, the proposed strategy achieves excellent results. To measure the performance of our heuristic strategy, we introduce the index

$$\eta = \frac{|\mathcal{C}^*(M)| - |\mathcal{C}^2(M)|}{|\mathcal{C}^*(M)|}$$

where $|\mathcal{C}^*(M)|$ is the optimal solution of our optimization problem computed leveraging on Algorithm 1 while $|\mathcal{C}^2(M)|$ is the solution provided by Heuristic Strategy 2. For $M \in [1\ 150]$, we found that the average of η, that is, $\langle\eta\rangle$ is equal to 0.025 while its standard deviation σ_η is equal to 0.015 which provides quantitative support to the evidence in Figure 5-2 suggesting that Heuristic strategy 2 is very capable of coping with the topology of the Cora citation network.

The Cora citation network is characterized by a giant SCC containing the majority of the network nodes that can be included in disjoint cycles. One could argue that this is the reason for which Heuristic Strategy 2 performs so well in our driver node selection problem as it includes these nodes in the set $\mathcal{C}(M)$ regardless of M. To explore this possibility, and hopefully dispel this doubt, we consider the Twitter Lists network [34, 17] the main topological features of which are resumed in Table 5-2

$\lvert\mathcal{V}\rvert$	23370
$\lvert\mathcal{P}\rvert$	33101
$\lvert\mathcal{S}\rvert$	23151
$\lvert\mathcal{R}\rvert$	421

Table 5-2: Main topological features of the Twitter Lists Network

Being much more sparse than the Cora citation network, the Twitter Lists network does not have a giant Strongly Connected Component. Moreover, the maximum number of nodes that can be included into disjoint cycles is 261 and these nodes are reasonably uniformly distributed among 62 SCCs. Thus, the advantage given by ensuring controllability of the largest SCC is neglectable for this network compared to the Cora citation Network. Nevertheless, as shown in Figure 5-3, Heuristic Strategy 2 still performs very well in the driver node selection task. This qualitative observation is supported by the evaluation of the index η. Namely, we have that $\langle\eta\rangle = 0.008$ and $\sigma_\eta = 0.012$ for M taken in the interval of integers

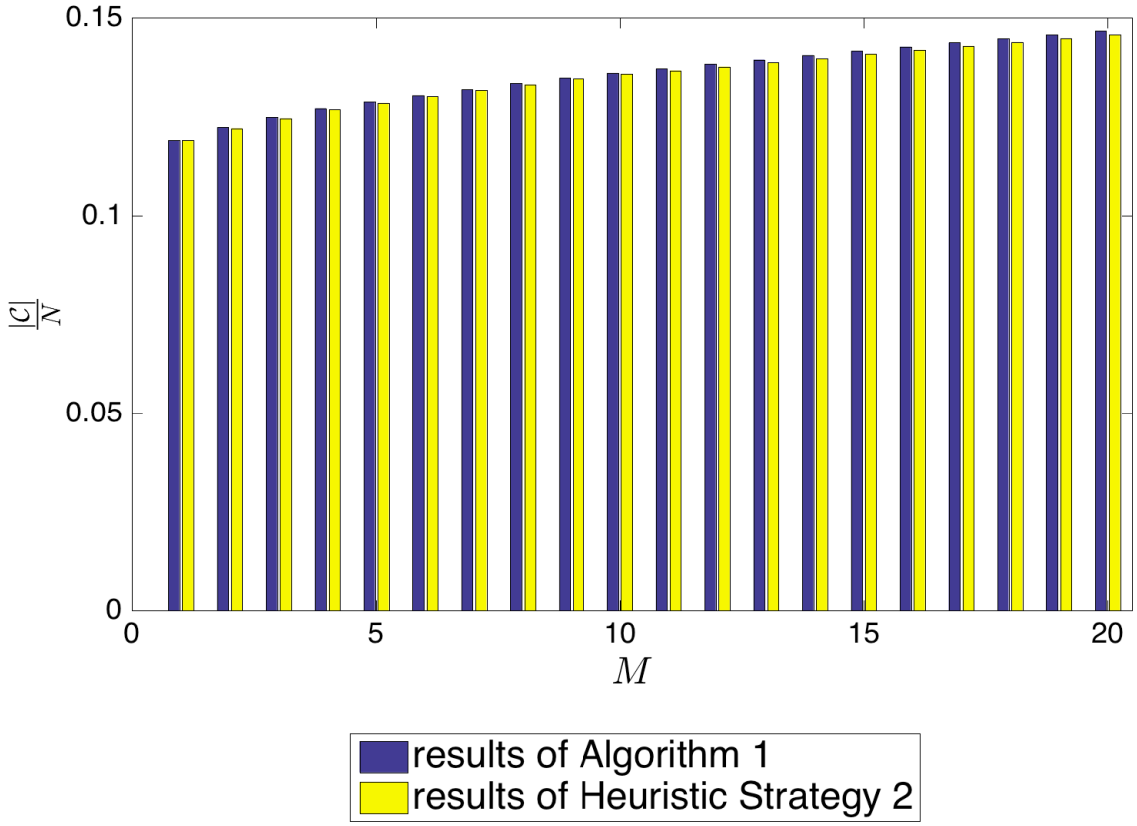

Figure 5-2: Plot of the fraction of the network nodes that can be made controllable over the number of driver nodes deployed M according to Algorithm 1 (blue) and Heuristic Strategy 2 (yellow) for the Cora citation network.

[0 150]. It is interesting to underline that although the number of RSCCS $|\mathcal{R}|$ of this network is 421, placing a driver in only 35 of these RSCCs is sufficient to guarantee all the network nodes that can be included into disjoint cycles are accessible from the drivers. Hence, from $M = 36$ on, also steps 25-33 of Heuristic Strategy 2 have been performed.

To provide further evidence on the performance of the proposed heuristic, we have analyzed two more networks, the main topological features of which are resumed in the Table **5-3** The structure of the DBLP citation network [35, 17] is characterized by a large number of small SCCs and the maximum number of nodes that can be included in disjoint cycles is 180, 66 of which in the same SCC. On the other hand, the B-cell Interactome network [33, 22] is characterized by a smaller amount of SCCs, one of which is a giant component composed of 3891 nodes. The maximum number of nodes of the B-cell interactome network

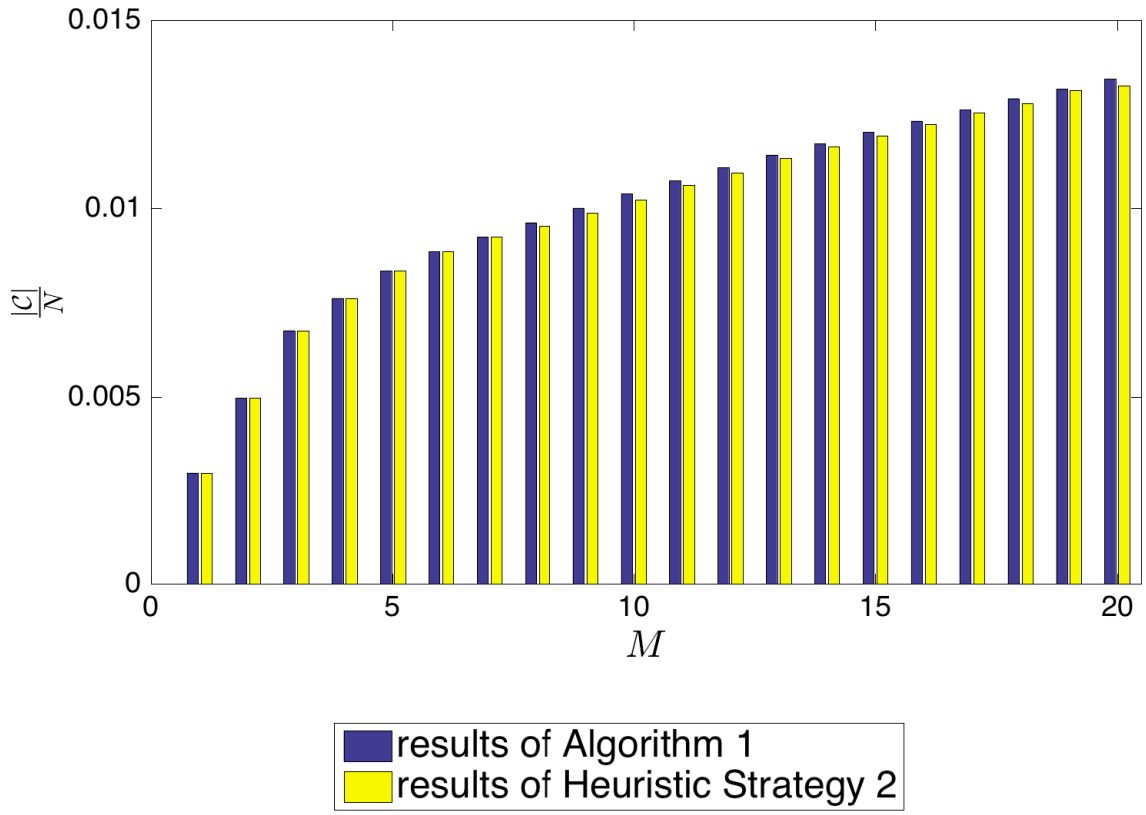

Figure 5-3: Plot of the fraction of the network nodes that can be made controllable over the number of driver nodes deployed M according to Algorithm 1 (blue) and Heuristic Strategy 2 (yellow) for the Twitter Lists network.

that can be included into disjoint cycles is 3670, 3610 of which lie in the giant component. As shown in Figure 5-4, Heuristic Strategy 2 performs very well also when coping with these two networks.

Again evaluating the index η provides further support to the evidence shown in Figure 5-4 as we have that for the DBLP citation network $\langle \eta \rangle = 0.003$ and $\sigma_\eta = 0.012$ while for the B-cell interactome, we find that $\langle \eta \rangle = \sigma_\eta = 0$ meaning that Heuristic Strategy 2 performs identically to the exact method provided in Algorithm 1.

Altogether, our numerical results show that Heuristic Strategy 2 performs very well when coping both with networks having a large number of nodes that can be included in disjoint cycles, as is the case for the B-cell Interactome network and the Cora citation network, as well as with networks for which the number of nodes that can be included in disjoint cycles

	B-cell	DBLP
$\lvert\mathcal{V}\rvert$	12591	5737
$\lvert\mathcal{P}\rvert$	49732	84892
$\lvert\mathcal{S}\rvert$	12286	1809
$\lvert\mathcal{R}\rvert$	1028	13

Table 5-3: Main topological features of the B-cell interactome and DBLP citation networks

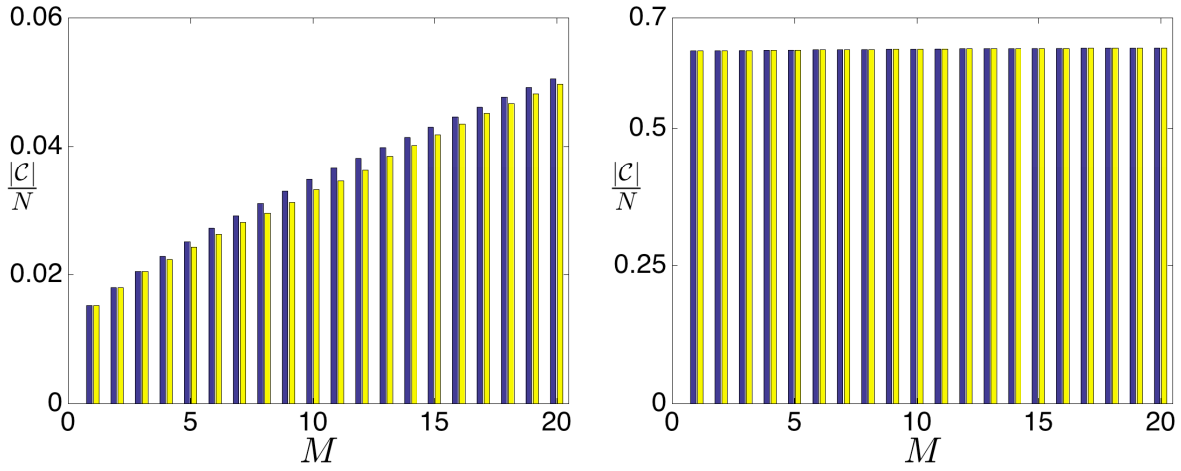

(a) (b)

Figure 5-4: Plot of the fraction of the network nodes that can be made controllable over the number of driver nodes deployed M according to Algorithm 1 (blue) and Heuristic Strategy 2 (yellow) for (a) the DBLP citation network and (b) the B-cell Interactome Network.

is smaller, as is the case for the DBLP citation network and the Twitter Lists network. While we were expecting this heuristic strategy to perform well when coping with cycle-rich networks as it is taylored to take advantage of the maximum possible number of nodes that can be included in disjoint cycles, its performance when coping with networks such as the DBLP citation or the Twitter Lists network is more surprising. We find an explanation to this empirical evidence in the fact that Heuristic Strategy 2 constrains the selection of $|D|$ drivers out of the nodes in the RSCCs of a network. As the nodes that have zero-indegree form RSCCs of their own, this is coherent with the signature on the optimal driver nodes described in Chapter 4. The fact that Heuristic Strategy 2 performs well when selecting driver nodes in networks for which the number of nodes that can be included in disjoint

cycles is not so large is encouraging as it fills the gap with Heuristic Strategy 1 which is expected to perform well only when the number of nodes in disjoint cycles is small. This ensures we have at our disposal a set of heuristic strategies that is expected to perform well regardless of the network topology.

CHAPTER 6

Partial Observability of Complex Networks

6.1 Observability of Dynamical Systems

According to the classical theory, a dynamical system is observable in a time interval $[t_0\ t_f]$ iff for all possible inputs and corresponding outputs it is possible to reconstruct its state its state in finite time [5]. As it is well known, observability and controllability are dual concepts. This implies that the controllability properties of a linear time invariant system

$$\begin{aligned} \dot{x} &= Fx + Bu \\ y &= Cx + Du \end{aligned} \tag{6-1}$$

can be deduced by studying the observability properties of its dual representation

$$\begin{aligned} -\dot{x} &= -F^T x - C^T u \\ y &= B^T x + D^T u. \end{aligned} \tag{6-2}$$

More formally, this means that the controllable subspace of the linear system in equation (6-1) is also the orthogonal complement of the unobservable subspace of its dual system in equation (6-2). The duality between controllability and observability has several practical implications. For instance, Kalman's rank test for controllability of the system in (6-2) provides the dimension of the observable subspace of the system in equation (6-1). It is for this reason that we compute the dimension of the observable subspace as the rank of the

well known observability matrix

$$O = \begin{bmatrix} C \\ CF \\ CF^2 \\ \dots \\ CF^{N-1} \end{bmatrix}$$

Consistently, applying the strucutral controllability theory to the dual representation of a dynamical system, we obtain that the generic dimension of the observable subspace can be computed by only inspecting the graph $\mathcal{G}(F^T, C^T)$ of the pair (F^T, C^T). In this graph, the nodes representing the input signals of the dual system actually represent the output signals of the real system. The generic dimension of the observable subspace is given by the number of edges of the largest stem-cycle disjoint subgraph of $\mathcal{G}(F^T, C^T)$ such that all stems originate in a node representing an input signal of the dual system, and all nodes of the stem-cycle disjoint subgraph are accessible, in $\mathcal{G}(F^T, B^T)$, from at least a node representing an input signal of the dual system.

6.2 Sensor Node Selection Strategies

As for the case of controllability, in the complex networks paradigm we can think of observability as a property to be conferred to a network. Lying in this perpective, the question arises of how to select a set of sensor nodes (the nodes where sensors are placed and from which the output signals are gathered) out of the set of network nodes so to confer some given observability properties to the network. The case of complete observability, assuming smooth nonlinear node dynamics has been studied by Liu et al. in [39]. Instead, as was the case for controllability, a toolbox of algorithms that cope with partial observability of complex networks is still lacking.

Given the duality between the concepts of controllability and observability, and the fact that we can also extend the results of the structural controllability theory to the concept of observability, we would be tempted to formulate the dual version of Lemma 3.2.1 which would allow us to extend all the results in Chapters 3 and 5 to sensor node selection problems. Unfortunately, this is not possible as given the observed dynamical network

$$\dot{x} = Fx \tag{6-3}$$

$$y = Cx \tag{6-4}$$

the dimension of its observable subspace does not coincide with the number of its observable nodes. We will illustrate this point by means of a simple example. Consider the simple network the graph of the dual representation of which is shown in Figure 6-1[1]. The observable

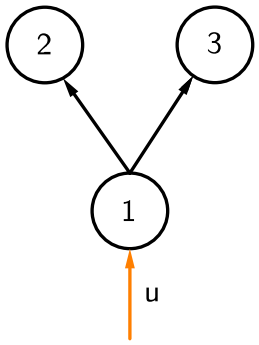

Figure 6-1: Graph of the dual representation of a very simple observed network.

subspace $\mathcal{O}$ is the linear span of the vectors $\mathbf{o_1} = [o_{11}\ 0\ 0]$ and $\mathbf{o_2} = [0\ o_{22}\ o_{23}]$, that is

$$\mathcal{O} = \{\lambda_1 \mathbf{o_1} + \lambda_2 \mathbf{o_2} \mid \lambda_1, \lambda_2 \in \mathbb{R}\} \tag{6-5}$$

and its projection onto the x_2, x_3 plane is the linear span of $\mathbf{k_2} = [0\ o_{22}\ o_{23}]$. As shown in Figure 6-2[2], if the free entries of the pair (F^T, C^T) vary, also the observable subspace does but its projection on the x_2, x_3 plane remains a straight line.
Roughly speaking, this means that in this case we can reconstruct the state of node v_1 together with the value of a linear combination of the states of nodes v_2 and v_3. As without additional information, neither the state of node v_2 nor the state of node v_3 can be reconstructed from knowledge of a linear combination of their value, we cannot consider either of the nodes observable. The practical implication is that the tools that can be used to select the driver nodes so to guarantee controllability of a fraction of the nodes of a complex network cannot be used to select the sensor nodes so to guarantee partial observability of a complex network. To develop such tools, we must start by understanding what are the graphical conditions that allow ensuring observability of only a fraction of the network nodes. We can do so by reasoning on the simple example in Figure 6-1. The reason for which the number of observable nodes does not coincide with the dimension of the observable subspace is that while the latter is equal to 2, the number of columns of the observability matrix containing a free entry is three. This implies that the projection of the observable subspace

[1] The fact that Figure 6-1 is identical to figure 3-1 is not accidental
[2] Again the fact that Figure 6-2 is identical to figure 3-2 is not accidental

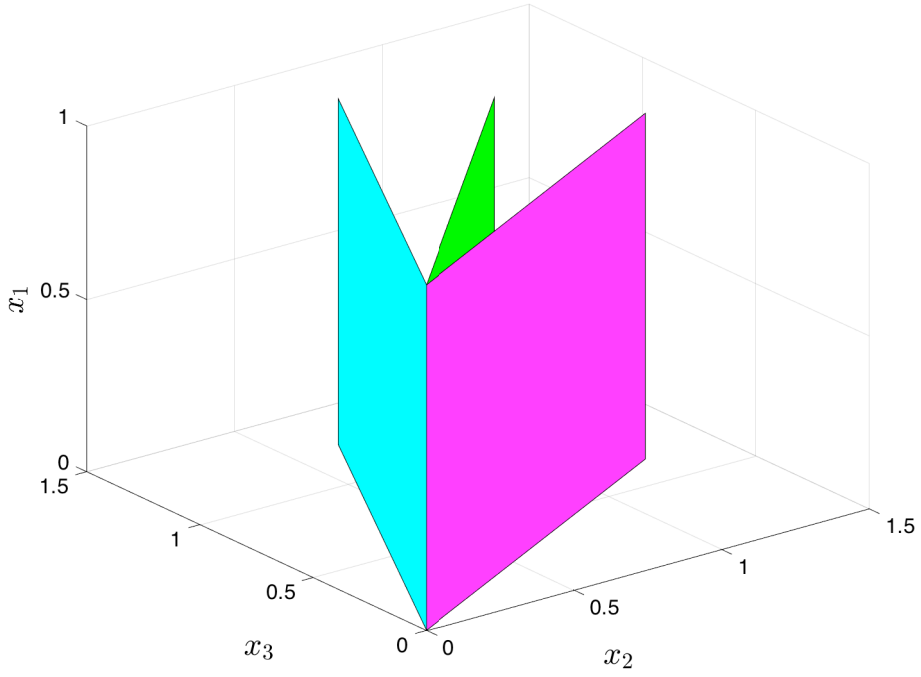

Figure 6-2: Plot of three different observable subspaces corresponding to three different sets of values of the free entries of the pair (F^T, C^T) for the controlled network portrayed in Fig. 3-1.

on the (x_2, x_3) plane is a straight line and does not correspond to $x_2 = 0$ nor to $x_3 = 0$. Hence, only a linear combination of the states of nodes v_2 and v_3 can be reconstructed. Generalizing, when the dimension of the observable subspace is smaller than the number of columns of the observability matrix that contain a free entry, the number of observable nodes is certainly smaller than the the dimension of the observable subspace. Hence, we can give the following condition

Lemma 6.2.1. *The number of observable nodes of a network coincides with the dimension of its observable subspace if and only if the number of columns of the observability matrix that include a nonzero entry is equal to the dimension of the observable subspace.*

Altough very clear, the condition provided by Lemma 6.2.1 is algebraic and thus can be efficiently be used only to test whether the number of observable nodes of a network coincides with the dimension of the observable subspace. Instead, leveraging it for the purpose designing a sensor node selection strategy is impractical. To do so, we revert to a graphical

approach and consider the observed network

$$\dot{x} = Ax \tag{6-6}$$

$$y = Cx \tag{6-7}$$

where once again, A is an adjacency matrix and each of its unit entries indicates a free entry in the matrix F in equation (6-3). As usual, we will denote by $\mathcal{G}$ the graph defined by the matrix A. Moreover, we also define the dual of the dynamical network in equation (6-6) as

$$-\dot{x} = A^T x - C^T u \tag{6-8}$$

and we denote by $\mathcal{G}^T$ the graph defined by the matrix A^T. As in this chapter we are interested in optimizing the observability properties of a network, we will name sensor nodes both the nodes of the network in equation (6-6) where the sensors are placed as well as the nodes of the dual network in equation (6-8) where the input signals u are injected.
Now, we can give the graphical condition equivalent to Lemma 6.2.1.

Lemma 6.2.2. *Consider the subgraph $\mathcal{G}_s^T$ of the graph $\mathcal{G}^T$ of the dual network in equation* (6-8) *composed of the nodes in the downstream of the sensor nodes and of all their connecting edges. The number of observable nodes of the network in equation* (6-6) *coincides with the dimension of its observable subspace if and only if there exists a stem-cycle disjoint subgraph of $\mathcal{G}_s^T$ including all of its nodes and such that the source node of each stem is a sensor node.*

Lemma 6.2.2 gives us a graphical condition to be verified that ensures a set of the network nodes is observable from a given set of sensor nodes. In what follows, we will leverage Lemma 6.2.2 to design sensor node selection strategies. The problem we will cope with is that of selecting, out of the entire set of network nodes, a set of sensor nodes that guarantee observability of the set controllable nodes $\mathcal{C}$ of a controlled network. We will thus assume that both the set Ω_D and $\mathcal{C}$ have been determined. The reason for which we decide to cope with this specific problem is twofold. First of all, in most applications where the complex network paradigm is deployed, the dynamics are only approximately known. For this reason, the robustness properties of feedback control strategies, where applicable, are appealing. As feedback control strategies rely on knowledge of the system state, observability of the controllable nodes is required, unless a sensor is placed on each of the latter. This brings us to the second point: we choose to determine the controllable nodes first, as thanks to the toolbox of algorithms developed in Chapters 3 and 5 this selection can be optimal (or suboptimal).

Our sensor node selection stategy is built in two steps. First, we guarantee that all the controllable nodes be in the upstream, in the graph $\mathcal{G}$, of at least a sensor node. This is done by determining the set of RSCCs of the graph $\mathcal{G}^T$ of minimum cardinality that ensures all the controllable nodes are accessible, in $\mathcal{G}^T$, from at least one of the selected RSCCs, and then placing a sensor in at least a node of each of these RSCCs. Then, we take the subgraph $\mathcal{G}_S^T$ of $\mathcal{G}T$ in the downstream of the selected sensor nodes and ensure it fulfills the conditions defined in Lemma 6.2.2 by selecting an additional set of sensor nodes. The steps required to deploy this sensor node selection strategy are described in the following algorithm.

Algorithm 3

1. Find the set of SCCs $\mathcal{S}$ of the graph $\mathcal{G}^T$.
2. Find the set of RSCCs $\mathcal{R} \subset \mathcal{S}$ of the graph $\mathcal{G}^T$.
3. Find the set of non root SCCs $S = \mathcal{S} - \mathcal{R}$.
4. Remove, from the set S all the SCCs that do not encompass a controllable node.
5. Find the set $R \subset \mathcal{R}$ of RSCCs that encompass at least a controllable node.
6. Associate a binary variable x_i to each element of $\mathcal{R}$.
7. Associate a set of binary variables z_{ij}, $j = 1, \ldots, |\mathcal{R}|$ to each element s_i of S. Namely, a binary variable z_{ij} is defined if the SCC s_i is in the downstream of the RSCC r_j.
8. Solve the following ILP:

$$\min \sum_j x_j \tag{6-9}$$

s.t.

$$z_{ij} - x_j = 0 \ \forall i, \ \forall j : \exists z_{ij} \tag{6-10}$$

$$-\sum_j z_{ij} \leq -1 \ \forall i \tag{6-11}$$

$$x_j = 1 \ \forall j : r_j \in \ R \tag{6-12}$$

9. $\mathcal{G}' = \mathcal{G}^T$.
10. Remove, from $\mathcal{G}'$ all the nodes that are neither i. associated to an RSCC r_j such that $x_j = 1$ or ii. in the downstream of an RSCC r_j such that $x_j = 1$;

11. Define the scalar $N = |\mathcal{V}'|$. N is equal to the number of nodes of the graph $\mathcal{G}'$ as of step 10.

12. Add, to $\mathcal{G}'$ a new node, say $N + 1$.

13. Add N new edges exiting node $N + 1$ and entering each node of $\mathcal{G}'$.

14. Add N new edges exiting each node of $\mathcal{G}'$ and entering node $N + 1$.

15. Associate a binary decision variable y_{ij} to each edge p'_{ij} of $\mathcal{G}'$.

16. Solve the following Integer Linear Program:

$$\min_{y} \quad \sum_{i} y_{i,N+1} \tag{6-13}$$

subject to

$$y_{ij} \in \{0,1\} \quad \forall i,j | p'_{ij} \in \mathcal{P}' \tag{6-14}$$

$$\sum_{j} y_{ij} = 1 \quad \forall i = 1,...,N \tag{6-15}$$

$$\sum_{i} y_{ij} = 1 \quad \forall j = 1,...,N \tag{6-16}$$

$$- \sum_{i:v_i \in r_j : x_j = 1} y_{i,N+1} \leq -1 \ \forall j : x_j = 1 \tag{6-17}$$

Again, while Algorithm 3 might seem convoluted, its rationale is very simple. In steps 1-5 we find all the SCCs that encompass a controllable node, and all the RSCCs of the graph $\mathcal{G}(A^T)$. Then, in steps 6-8 we ensure each controllable node be in the downstream (in $\mathcal{G}(A^T)$) of at least a sensor node. This is done by associating a variabile x_j to each RSCC of $\mathcal{G}^T$, and a set of variables z_{ij} to each SCC s_i that encompasses at least a controllable node. The existence of the variable z_{ij} implies that the SCC s_i is in the downstream of the RSCC r_j. Then by solving the ILP in equations (6-9)-(6-12), the minimal set of RSCCs that have all the controllable nodes in their downstream is selected. Namely, if $x_i = 1$ then the RSCC r_i will include a sensor node. Equation (6-9) ensures the selected set is minimal, equations (6-10) and (6-11) guarantee all non root SCCs that encompass a controllable node be in the downstream of a selected RSCC, and equation (6-12) makes sure that all the RSCCs that encompass controllable nodes also include a sensor node.

Steps 1-5 can be viewed as the construction of a two level graph where all the RSCCs are source nodes and thus constitute the first level of this new graph and all the SCCs are sink nodes and thus constitute the second level. The ILP in equations (6-9)-(6-12) then selects

the minimal set of sources of this two-level graph such that i. all sink nodes associated to SCCs of $\mathcal{G}^T$ that encompass a controllabe node are in the downstream of a selected source and ii. all the sources associated to RSCCs that encompass a controllable node are selcted. Once we have ensured each controllable node is in the downstream (in $\mathcal{G}^T$) of at least a sensor node, we must ensure the downstream of the latters is stem-cycle disjoint with each stem originating from a sensor node. This is done in steps 9-16 by adding an additional set of sensor nodes. Namely, in step 9 and 10 we start building an augmented graph $\mathcal{G}'$ by eliminating, from the graph $\mathcal{G}^T$, all the nodes that are not in the selected RSCCs or in their downstream. Then, in steps 12-14 we add an additional node representing the sensors to be placed, and connect it to all the nodes of $\mathcal{G}'$. In step 15, we associate a binary variable y_{ij} to each edge of the augmented graph $\mathcal{G}'$ and finally in step 16 we find the minimal set of sensor nodes such that the downstream of the RSCCs selected in step 8 is stem-cycle disjoint, with each stem originating from a sensor node. As was the case in Algorithm 1, this is done by finding a cycle partition of the graph $\mathcal{G}'$. This time, as implied by equation (6-13), we seek for the cycle partition that minimizes the number of edges exiting from node $N+1$. As if $y_{i,N+1} = 1$ then node i is a sensor node, this means minimizing the number of additional sensor nodes deployed.

6.3 Computational Considerations

As the reader can note, Algorithm 3 encompasses two ILPs. Given the considerations made in chapter 3 a legitimate question to ask is whether these are NP-hard. Let us start from the second ILP, that in equations (6-13)-(6-17). We note that all constant terms are integer and that the matrix defined by the constraints is binary. Hence, we must only prove that we can decompose it into two blocks I_1 and I_2 as prescribed by Lemma 2.2.1. We already know that the constraints in equations (6-15) and (6-16) will fall into the same block, say I_1, as they are the usual constraints used to find a cycle partition. The matrix defined by the constriaint in equation (6-17) can fall in either block. In any case, it will not violate any of the prescriptions in Lemma 2.2.1 as the variables that appear in its expression do not appear in the other constraints. Hence the ILP in equations (6-13)-(6-17) is not NP-hard.
Now, we can turn our attention to the first ILP, that in equations (6-9)-(6-12). Once more, the known terms of the constraints are integer and the elements of the constraint matrix only take the values of $\{-1,\ 0,\ 1\}$ and thus it is worthwile checking if the constraint matrix fulfills the sufficient condition for total unimodularity given in Lemma 2.2.1. If we choose to include the matrix defined by the constraint in equation (6-10) in block I_1 and the matrix defined

by the constraints in equations (6-12) and (6-11) in block I_2 we note that each variable z_{ij} appears once in block I_1 and once in block I_2 with opposite sign and the same applies to each variable x_j. Hence, the matrix defined by the constraints in equations (6-10)-(6-12) can be decomposed as prescribed by Lemma 2.2.1 and thus also the first ILP in Algorithm 3 is not NP-hard guaranteeing that Algorithm 3 can be deployed in polynomial time.

CHAPTER 7

Conclusions

Real world complex systems are not built to be controlled. Power grids, biological networks, financial markets and social networks have developed without taking into explicit account the need to control them. Hence, to control them efficiently, an accurate selection of the nodes where input signals must be injected is required. As anticipated, we can translate this problem into a different concept of controllability: from a structural property that a dynamical system can, or cannot have, to a feature that must be conferred to some or all the network nodes. From a theoretical point of view, this poses a new challenge, as the classical tools of control theory must be complemented with driver node selection algorithms. In the last five years, researchers from the engineering and physics community have promptly responded to this challenge, as the problem of ensuring complete controllability of complex networks has been vastly studied. Several papers have been published on this topic on some of the most prestigious scientific journals. Perhaps, the most popular approach has been that of leveraging the structural controllability theory to develop driver node selection strategies to ensure complete controllability of complex networks. With the toolobox of algorithms presented in this thesis, we have generalized this approach to the more realistic scenario in which controllability is sought of only a fraction of the network nodes. We have translated this shift of perspective into two optimization problems, a first one in which a set of driver nodes of fixed cardinality must is selected in order to maximize the number of controllable nodes of a network, and a second one in which the minimal set of driver nodes is sought that allows ensuring structural controllability of a well-defined subset of the network nodes. In this thesis we have presented optimal and suboptimal but computationally efficient driver node selection algorithms capable of coping with the presented optimization problems. Then, leveraging these tools, we have studied the relation between the network structure and its readiness to be controlled, ultimately developing an index, the structural

permeability of complex networks to control signals, capable of measuring the ease with which a network can be made controllable regardless of the number of driver nodes deployed for the task. Finally, we have complemented the driver node selection algorithms with sensor node selection strategies in order to ensure being able to deploy feedback control strategies. This thesis has the ambition of capping off the topic of structural controllability of complex networks in it generalizes the approaches found in the literature which are mainly related to ensuring complete controllablity. We close this thesis by providing the reader with an outlook on the current lines of reasearch that are currently under investigation on the topic of controllability of complex networks.

7.1 Open problems and Future Work

In an effort to come closer to actually controlling complex networks, recently, researchers have started to focus on measuring the effort required to control complex dynamical networks. Taking different approaches [62], [64] [48], different studies have found that the worst-case effort required to achieve a control goal grows exponentially with the ratio between the driver nodes and the number of nodes of the network. In some sense this is not surprising, as what allows indirectly controlling a network node, that is, the edges that link it to other nodes, also introduces a dependency of its dynamics with respect to that of the nodes to which it is connected. The results in these papers seem to suggest that although theretically possibile, it is inpractical to control a number of nodes that is significantly larger than the number of drivers deployed for the task. The viewpoint taken in this thesis is that to control a number of nodes that is significantly larger than the number of drivers with reasonable energy, the latters must be selected explicitly taking into account the control goal to be accomplished. The idea is that, varying the the selected set of drivers nodes also changes the paths, that is, the sequence of edges edges, through which the control signals will permeate through the network. These paths determine the dependecies that will arise between the controlled dynamics of the network nodes. Roughly speaking, we can imagine driver node selection strategies that aim at exploiting the dependecies introduced by the network edges that facilitate achieving the desired control goals while avoiding the selection, as drivers, of the nodes that would make sure some undesired dependecies come into play. Indeed, this can be a promising line of research that allows us to design driver node selection strategies that can bring us close to actually controlling real world complex systems.

Bibliography

[1] Marian Anghel, Kenneth A Werley, and Adilson E Motter. Stochastic model for power grid dynamics. In *System Sciences, 2007. HICSS 2007. 40th Annual Hawaii International Conference on*, pages 113–113. IEEE, 2007.

[2] Alex Arenas, Albert Díaz-Guilera, Jurgen Kurths, Yamir Moreno, and Changsong Zhou. Synchronization in complex networks. *Physics Reports*, 469(3):93–153, 2008.

[3] Albert-László Barabási et al. Scale-free networks: a decade and beyond. *science*, 325(5939):412, 2009.

[4] Dongbo Bu, Yi Zhao, Lun Cai, Hong Xue, Xiaopeng Zhu, Hongchao Lu, Jingfen Zhang, Shiwei Sun, Lunjiang Ling, Nan Zhang, et al. Topological structure analysis of the protein–protein interaction network in budding yeast. *Nucleic acids research*, 31:2443–2450, 2003.

[5] Frank M Callier and Charles A Desoer. *Linear Systems Theory*. Springer, 1991.

[6] Fei Chen, Zengqiang Chen, Linying Xiang, Zhongxin Liu, and Zhuzhi Yuan. Reaching a consensus via pinning control. *Automatica*, 45(5):1215–1220, 2009.

[7] FG Commoner. A sufficient condition for a matrix to be totally unimodular. *Networks*, 3(4):351–365, 1973.

[8] Pietro DeLellis, Franco Garofalo, Francesco Lo Iudice, and Elena Napoletano. Wealth distribution across communities of adaptive financial agents. *New Journal of Physics*, 17(8):083003, 2015.

[9] Pietro DeLellis, Franco Garofalo, Francesco Lo Iudice, and Giovanni Mancini. Decentralised coordination of a multi-agent system based on intermittent data. *International Journal of Control*, 88(8):1523–1532, 2015.

[10] Giovanni Filatrella, Arne Hejde Nielsen, and Niels Falsig Pedersen. Analysis of a power grid using a kuramoto-like model. *The European Physical Journal B*, 61(4):485–491, 2008.

[11] Prasanna Gai and Sujit Kapadia. Contagion in financial networks. In *Proceedings of the Royal Society of London A: Mathematical, Physical and Engineering Sciences*, page rspa20090410. The Royal Society, 2010.

[12] Marco Galbiati, Danilo Delpini, and Stefano Battiston. The power to control. *Nature Physics*, 9(3):126–128, 2013.

[13] Jianxi Gao, Yang-Yu Liu, Raissa M D'Souza, and Albert-László Barabási. Target control of complex networks. *Nature communications*, 5, 2014.

[14] K.-I. Goh, B. Kahng, and D. Kim. Universal behavior of load distribution in scale-free networks. *Phys. Rev. Lett.*, 87:278701, Dec 2001.

[15] J. Silvio Gutkind. Regulation of mitogen-activated protein kinase signaling networks by g protein-coupled receptors. *Sci. STKE*, 2000(40):re1, 2000.

[16] S. Hosoe. Determination of generic dimensions of controllable subspaces and its application. *Automatic Control, IEEE Transactions on*, 25(6):1192–1196, Dec 1980.

[17] http://konect.uni koblenz.de/networks.

[18] http://moreno.ss.uci.edu.

[19] http://research.mssm.edu/maayan/datasets.

[20] http://toreopsahl.com/datasets/.

[21] http://vlado.fmf.uni lj.si/pub/networks/data/bio/foodweb/foodweb.htm. Pajek's dataset.

[22] http://wiki.c2b2.columbia.edu/califanolab.

[23] http://wws.weizmann.ac.il/mcb/UriAlon/download/collection-complex networks.

[24] http://www3.nd.edu/ networks/resources/metabolic/index.html. Barabasilab dataset of metabolic networks.

[25] http://www.wormatlas.org.

[26] Ramon Ferrer i Cancho, Christiaan Janssen, and Ricard V Solé. Topology of technology graphs: Small world patterns in electronic circuits. *Physical Review E*, 64(4):046119, 2001.

[27] R. Kalman. Mathematical description of linear dynamical systems. *Journal of the Society for Industrial and Applied Mathematics Series A Control*, 1(2):152–192, 1963.

[28] Stuart A Kauffman. Metabolic stability and epigenesis in randomly constructed genetic nets. *Journal of theoretical biology*, 22(3):437–467, 1969.

[29] Wesley K. Kroeze, Douglas J. Sheffler, and Bryan L. Roth. G-protein-coupled receptors at a glance. *Journal of Cell Science*, 116(24):4867–4869, 2003.

[30] Harold William Kuhn, Albert William Tucker, and George Bernard Dantzig. *Linear inequalities and related systems*. Number 38. Princeton university press, 1956.

[31] Aud Larsen, Jorun K Egge, Jens C Nejstgaard, Iole Di Capua, Runar Thyrhaug, Gunnar Bratbak, and T Frede Thingstad. Contrasting response to nutrient manipulation in arctic mesocosms are reproduced by a minimum microbial food web model. *Limnology and oceanography*, 60(2):360–374, 2015.

[32] Ernest Bruce Lee and Lawrence Markus. Foundations of optimal control theory. Technical report, DTIC Document, 1967.

[33] Celine Lefebvre, Wei Keat Lim, Katia Basso, Riccardo Dalla Favera, and Andrea Califano. A context-specific network of protein-dna and protein-protein interactions reveals new regulatory motifs in human b cells. In *Systems Biology and Computational Proteomics*, pages 42–56. Springer, 2007.

[34] Jure Leskovec and Julian J Mcauley. Learning to discover social circles in ego networks. In *Advances in neural information processing systems*, pages 539–547, 2012.

[35] Michael Ley. The dblp computer science bibliography: Evolution, research issues, perspectives. In *String Processing and Information Retrieval*, pages 1–10. Springer, 2002.

[36] Ching-Tai Lin. Structural controllability. *Automatic Control, IEEE Transactions on*, 19(3):201–208, Jun 1974.

[37] Yang-Yu Liu, Jean-Jacques Slotine, and Albert-Laszlo Barabasi. Controllability of complex networks. *Nature*, 473(7346):167–173, 2011.

[38] Yang-Yu Liu, Jean-Jacques Slotine, and Albert-Laszlo Barábasi. Control centrality and hierarchical structure in complex networks. *PLoS ONE*, 7(9):e44459, 09 2012.

[39] Yang-Yu Liu, Jean-Jacques Slotine, and Albert-László Barabási. Observability of complex systems. *Proceedings of the National Academy of Sciences*, 110(7):2460–2465, 2013.

[40] Francesco Lo Iudice, Franco Garofalo, and Francesco Sorrentino. On the observability of the largest set of controllable nodes of complex networks. 2016.

[41] Thomas Lux and Michele Marchesi. Scaling and criticality in a stochastic multi-agent model of a financial market. *Nature*, 397(6719):498–500, 1999.

[42] H Maeda, G Y Bharate, and J Daruwalla. Polymeric drugs for efficient tumor-targeted drug delivery based on epr-effect. *European Journal of Pharmaceutics and Biopharmaceutics*, 71(3):409 – 419, 2009.

[43] Susanna C Manrubia, Alexander S Mikhailov, et al. *Emergence of dynamical order: synchronization phenomena in complex systems*, volume 2. World Scientific, 2004.

[44] Maria Julia Marinissen and J Silvio Gutkind. G-protein-coupled receptors and signaling networks: emerging paradigms. *Trends in Pharmacological Sciences*, 22(7):368 – 376, 2001.

[45] Marc Mézard and Giorgio Parisi. The bethe lattice spin glass revisited. *The European Physical Journal B-Condensed Matter and Complex Systems*, 20(2):217–233, 2001.

[46] Tamás Nepusz and Tamás Vicsek. Controlling edge dynamics in complex networks. *Nature Physics*, 8(7):568–573, 2012.

[47] R. Olfati-Saber. Flocking for multi-agent dynamical systems: algorithms and theory. *IEEE Trans. Autom. Contr.*, 51:401–419, 2006.

[48] Fabio Pasqualetti, Sandro Zampieri, and Francesco Bullo. Controllability metrics, limitations and algorithms for complex networks. *Control of Network Systems, IEEE Transactions on*, 1(1):40–52, 2014.

[49] S. Poljak. On the generic dimension of controllable subspaces. *Automatic Control, IEEE Transactions on*, 35(3):367–369, Mar 1990.

[50] Maurizio Porfiri, D Gray Roberson, and Daniel J Stilwell. Tracking and formation control of multiple autonomous agents: A two-level consensus approach. *Automatica*, 43(8):1318–1328, 2007.

[51] Wei Ren. Consensus strategies for cooperative control of vehicle formations. *Control Theory & Applications, IET*, 1(2):505–512, 2007.

[52] Wei Ren and Randal W Beard. *Distributed consensus in multi-vehicle cooperative control*. Springer, 2008.

[53] Craig W Reynolds. Flocks, herds and schools: A distributed behavioral model. In *ACM SIGGRAPH computer graphics*, volume 21, pages 25–34. ACM, 1987.

[54] Sara Brin Rosenthal, Colin R Twomey, Andrew T Hartnett, Hai Shan Wu, and Iain D Couzin. Revealing the hidden networks of interaction in mobile animal groups allows prediction of complex behavioral contagion. *Proceedings of the National Academy of Sciences*, 112(15):4690–4695, 2015.

[55] Justin Ruths and Derek Ruths. Control profiles of complex networks. *Science*, 343(6177):1373–1376, 2014.

[56] Robert W Shields and J Boyd Pearson. Structural controllability of multi-input linear systems. *Rice University ECE Technical Report*, (TR7502), 1975.

[57] Brian Skyrms and Robin Pemantle. A dynamic model of social network formation. In *Adaptive Networks*, pages 231–251. Springer, 2009.

[58] Francesco Sorrentino, Mario di Bernardo, Franco Garofalo, and Guanrong Chen. Controllability of complex networks via pinning. *Phys. Rev. E*, 75:046103, Apr 2007.

[59] Steven H Strogatz. Exploring complex networks. *Nature*, 410(6825):268–276, 2001.

[60] Lovro Šubelj and Marko Bajec. Model of complex networks based on citation dynamics. In *Proceedings of the 22nd international conference on World Wide Web companion*, pages 527–530. International World Wide Web Conferences Steering Committee, 2013.

[61] Tyler Summers, Fabrizio Cortesi, and John Lygeros. On submodularity and controllability in complex dynamical networks. 2014.

[62] Jie Sun and Adilson E Motter. Controllability transition and nonlocality in network control. *Physical review letters*, 110(20):208701, 2013.

[63] Robert Tarjan. Depth-first search and linear graph algorithms. *SIAM journal on computing*, 1(2):146–160, 1972.

[64] Gang Yan, Georgios Tsekenis, Baruch Barzel, Jean-Jacques Slotine, Yang-Yu Liu, and Albert-Laszlo Barabasi. Spectrum of controlling and observing complex networks. *Nature Physics*, 11:779–786, 2015.

[65] Wenwu Yu, Guanrong Chen, Jinhu Lu, and Jurgen Kurths. Synchronization via pinning control on general complex networks. *SIAM Journal on Control and Optimization*, 51(2):1395–1416, 2013.

[66] Zhengzhong Yuan, Chen Zhao, Zengru Di, Wen-Xu Wang, and Ying-Cheng Lai. Exact controllability of complex networks. *Nature communications*, 4, 2013.

[67] Lenka Zdeborová and Marc Mézard. The number of matchings in random graphs. *Journal of Statistical Mechanics: Theory and Experiment*, 2006(05):P05003, 2006.

[68] Ranran Zhang, Mithun Vinod Shah, Jun Yang, Susan B. Nyland, Xin Liu, Jong K. Yun, Reka Albert, and Thomas P. Loughran. Network model of survival signaling in large granular lymphocyte leukemia. *Proceedings of the National Academy of Sciences*, 105(42):16308–16313, 2008.